Identification of microRNA-27a as a key regulator of cholesterol homeostasis

by

Abrar A. Khan[1], Vinayak Gupta[1], Kalyani Ananthamohan[1], Vikas Arige[1], S. Santosh Reddy[2], Manoj K. Barthwal[2], Madhu Dikshit[2], G. Bhanuprakash Reddy[3], Nitish R. Mahapatra[1]

from the

[1]Department of Biotechnology, Bhupat and Jyoti Mehta School of Biosciences, Indian Institute of Technology Madras, Chennai 600036, India
[2]Pharmacology Division, Academy of Scientific and Innovative Research (AcSIR), CSIR-Central Drug Research Institute, Lucknow 226031, India
[3]National Institute of Nutrition, Jamia Osmania PO, Hyderabad 500007, India

Short title: Regulation of HMG-CoA reductase by miR-27a

Word Count: 11890**,**

Word Count of Abstract: 286**,**

Number of Figures: 10

Address for correspondence:

Dr. N. R. Mahapatra, Department of Biotechnology, Bhupat and Jyoti Mehta School of Biosciences, Indian Institute of Technology Madras, Chennai 600036, India. Tel: 91-44-2257-4128; E-mail: nmahapatra@iitm.ac.in

ABSTRACT

3-Hydroxy-3-methylglutaryl-coenzyme A reductase gene (*Hmgcr*) that codes for the rate-limiting enzyme in the cholesterol biosynthesis pathway is a key modulator of dyslipidemia and consequent cardiovascular diseases. However, mechanism of regulation of *Hmgcr*, especially at the post-transcriptional level, is poorly understood. *In silico* predictions coupled with systematic functional analysis revealed specific interactions of miR-27a with mouse *Hmgcr* 3'-UTR in mouse and human hepatocytes. In corroboration, miR-27a expression negatively correlated with *Hmgcr* transcript level in various cultured cell lines as well as rodent and human tissues. Hmgcr protein level also displayed inverse correlation with miR-27a level in liver tissues of several rodent models of metabolic disorders (viz. genetically hypertensive blood pressure high *vs*. genetically hypotensive blood pressure low mice, spontaneously hypertensive rats *vs*. Wistar Kyoto rats, and rats fed with high fat and fructose diet *vs*. rats fed with a normal chow diet). Consistently, ribonucleoprotein immunoprecipitation assays using antibodies against Ago2 and human hepatocyte HuH-7 cells over-expressing miR-27a revealed enrichment of *HMGCR* in the Ago2-immunoprecipitated fraction. Of note, cholesterol depletion in mouse hepatocyte AML-12 cells down-regulated endogenous miR-27a and augmented Hmgcr protein level; exogenous cholesterol treatment enhanced miR-27a with concomitant reduction in the Hmgcr protein level. Computational analysis of the proximal 1 kb promoter region of mmu-miR-27a predicted multiple Egr1 binding sites; corroboratively, over-expression/down-regulation of Egr1 augmented/diminished the miR-27a promoter activity in AML12 cells and chromatin immunoprecipitation (ChIP) assays confirmed *in vivo* interaction of Egr1 with the mmu-miR-27a promoter regions. Hypoxic stress augmented miR-27a and Egr1 expression in AML-12 cells; ChIP assays revealed enhanced binding of Egr1 with miR-27a promoter during hypoxia. Taken together, this study provides evidence for post-transcriptional regulation of *Hmgcr* by miR-27a under basal/pathophysiological conditions and has implications for understanding the mechanisms of cholesterol homeostasis.

INTRODUCTION

Cardiovascular disease (CVD) remains the leading cause of global mortality and morbidity (1) despite extensive research over the past several decades. Among various determinants of CVD plasma concentration of cholesterol is an important one as dyslipidemia (deregulated lipid and lipoprotein metabolism) may lead to multiple disease states including atherosclerosis, coronary artery disease, obesity, hypertension and type 2 diabetes (2-4). 3-hydroxy-3-methylglutaryl-coenzyme A (HMG-CoA) reductase gene (human: *HMGCR*, mouse/rat: *Hmgcr*) that codes for a ~ 97 kDa endoplasmic-reticulum membrane glycoprotein and catalyzes the rate-limiting step (HMG-CoA to mevalonate) in the cholesterol biosynthesis pathway (5-7) is, therefore, a logical modulator of dyslipidemia and its consequent CVD. Accordingly, statin drugs targeting HMG-CoA reductase are widely used to reduce high cholesterol levels and risk of CVD (8,9).

HMGCR gene is located on q arm of 5th and 13th chromosome in human and mouse, respectively. Several studies reported associations of SNPs in the *HMGCR* locus (viz. rs12654264, rs3846662, rs7703051, rs5908 rs12916, rs17238540 and rs3846663) with level of total cholesterol, LDLc and risk for dyslipidemia/stroke/blood pressure and coronary heart disease (10-18). Efficacy of statins is influenced by a haplotype consisting of three intronic single nucleotide polymorphisms (SNPs) (viz. rs17244841, rs3846662, and rs17238540) in *HMGCR* because this haplotype leads to an alternatively spliced *HMGCR* transcript that is less sensitive to simvastatin/pravastatin inhibition (19-21).

HMGCR expression/enzyme activity is highly regulated by feedback control mechanisms involving sterols and nonsterol (end-products of mevalonate metabolic pathway) at transcriptional and post-translational levels by family of sterol regulatory element binding proteins (SREBPs), SREBP cleavage activated protein (SCAP), and insulin induced genes (Insig1 and Insig2) (7). Interestingly, *HMGCR* expression is down-regulated by hypoxia due to accumulation of lanosterol and hypoxia-inducible factor-1α (HIF-1α)

dependent induction of Insigs (22). However, the molecular mechanism regulating mouse *Hmgcr* (*Hmgcr*) expression at the post-transcriptional level is poorly understood.

microRNAs (miRNAs) are a class of small noncoding RNAs that control gene expression by directing their target mRNAs for degradation and/or translational repression (23). Dysregulation in the miRNA function may lead to various human diseases including cardiovascular and metabolic disorders (24-26). Indeed, recent studies have revealed that miRNAs play important roles in cardiovascular development, physiology, and pathophysiology (27-29). We undertook systematic computational and extensive experimental analyses that revealed crucial roles for miR-27a to govern the *Hmgcr* gene expression. In addition, this study, for the first time, provided evidence of post-transcriptional regulation of *Hmgcr* expression under pathophysiological conditions, including hypoxia by miR-27a. This study also highlights the previously unknown role of Egr1 in the regulation of miR-27a expression.

MATERIALS AND METHODS.

Lipid-related QTLs and LOD scores.

For comparative genomic analysis, the data pertaining to lipid-related QTLs, their respective LOD scores, and all the genes with their respective positions in a particular QTL was mined from the Rat Genome Database (Supplementary Table 2).

Sequence comparison using VISTA.

Mouse and rat *Hmgcr* gene sequences (GenBank accession no: NM_008255, and NM_ NM_013134.2 respectively) were retrieved from UCSC genome browser (http://www.genome.ucsc.edu/). Visualization Tools for Alignments (VISTA) was used to plot the graph indicating the degree of homology between mouse and rat *Hmgcr*. Specifically, we used mVISTA browser which relies on

AVID alignment algorithm that uses global alignment for sequence comparision of the input queries (Supplementary Table 2).

In silico prediction of potential miRNA binding sites in mouse *Hmgcr*-3′UTR.

Mouse Hmgcr (*Hmgcr*)-3'UTR sequence (NCBI reference number: NM_008255.2) was downloaded from the UCSC genome browser and analyzed using multiple bioinformatic algorithms [viz. miRWalk , miRanda , TargetScan , PITA , RNA22 , and RNAhybrid (Supplementary Table 2)] to predict miRNA target sites. Since, a large number of miRNAs were predicted by these online tools, we selected only those miRNAs that were predicted by at least five algorithms. Further, differences in hybridization free energy indicating the stability of the microRNA-mRNA interaction was determined computationally by two online tools called PITA and RNAhybrid. The lower or more negative $\Delta\Delta G$ value predicted by PITA represents the stronger binding of the microRNA to the given site; as a rule of thumb, sites having $\Delta\Delta G$ values below -10 are likely to be functional. The RNA hybrid calculates the minimum free energy (ΔG) of hybridizations of target mRNA and miRNA.

Tissue-specific expression of endogenous *HMGCR* and has-miR-27a-3p levels.

HMGCR expression data in various human tissues was mined from the GTEx portal (Supplementary Table 2). Likewise, tissue-specific hsa-miR-27a-3p expression was obtained from miRmine and DASHR (Supplementary Table 2), respectively. Only tissues common to the GTEx portal and DASHR or miRmine were chosen for correlation analysis. The data was normalized to a particular tissue in each set of analysis and expressed as fold change. In brief, the expression data from miRmine and GTEx was normalized to pancreas while the expression in spleen was used for normalizing expression profiles from DASHR.

Generation of mouse Hmgcr 3'-UTR/luciferase and mmu-miR-27a promoter/luciferase reporter constructs.

The mouse Hmgcr 3'-UTR domain (+20359/+21975 bp) was PCR-amplified using Phusion® High Fidelity DNA Polymerase (Finnzymes), mouse genomic DNA (Jackson Laboratory, Bar Harbor, USA) and gene specific primers (FP: 5'-CGT**GCTAGC**GGATCCTGACACTGAACTG-3', RP: 5'-GC**GGCCGGCC**TTCAATGTTAACTTCCTTTC -3') as designed by primer 3 (Supplementary Table 2). The numberings of the nucleotide positions are with respect to cap site as +1 position. Bold and underlined nucleotides in forward and reverse primers are the restriction sites for *Nhe* I and *Fse* I, respectively, that were added for cloning of the PCR-amplified 3'-UTR into the firefly-luciferase expressing pGL3-promoter reporter vector (Promega). The purified Hmgcr3'-UTR PCR product was cloned between *Xba* I and *Fse* I sites of pGL3-Promoter vector because *Nhe* I digested PCR product had compatible ends for *Xba* I-digested pGL3-promoter reporter vector. Of note, *Fse* I is a unique site present in the pGL3-promoter vector after *Xba* I site at 1949-1953 bp. Authenticity of the Hmgcr 3'-UTR reporter plasmid was confirmed by DNA sequencing using pGL3-promoter vector sequencing primers [forward primer (1782-1801bp): 5′-CGTCGCCAGTCAAGTAACAA-3′ and reverse primer (2118–2137bp): 5′-CCCCCTGAACCTGAAACATA-3′)].

To abrogate the binding of miRNAs, 3'UTR-deletion construct was generated using site-directed mutagenesis wherein the putative miR-27a binding sites were deleted. The 3'UTR-deletion construct for miR-27a was generated by using the wild-type Hmgcr-3'UTR-reporter construct as template and the following primers: forward, 5' CGCGGGCATTGGGTTCTCAATTAAAAATCTCAATGCACT-3' and reverse, 5'-AGTGCATTGAGATTTTTAATTGAGAACCCAATGCCCGCG-3'. This deletion in the reporter plasmid was confirmed by DNA sequencing and the resultant construct was named as m*Hmgcr* 27a mut 3'-UTR.

To generate the mmu-miR-27a promoter/luciferase reporter construct, -1079 bp to +26 bp region of the miR-27a promoter was PCR-amplified using mouse genomic DNA as described above and primers (forward, 5'-CTA**GCTAGC**AACTTTAACTGGCACGCAGG-3', and reverse, 5'-CCG**CTCGAG**GGCATCAAATCCCATCCC-3'). Bold and underlined nucleotides in forward and reverse primers are the restriction sites for *Nhe* I and *Xho* I, respectively, that were added for cloning of the PCR-amplified miR-27a promoter region into the pGL3-basic vector (Promega). The accuracy of resultant construct was confirmed by DNA sequencing.

Generation of microRNA expression plasmids.

To generate plasmid expressing miR-27a the sequence of the pre-miRNA was retrieved from miR-Base/UCSC genome browser, PCR-amplified using mouse genomic DNA as template and gene specific primers [miR-27a-FP: 5'-CGC**GGATCC**TCGCCAAGGATGTCTGTCTT-3', miR-27a-RP: 5'-CCG**CTCGAG**GTTTCAGCTCAGTAGGCACG-3']. Bold and underlined nucleotides are *BamH* I and *Xho* I restriction sites that were added to the forward and reverse primers, respectively. The purified PCR-amplified DNA was cloned between *BamH* I and *Xho* I restriction sites in the pcDNA3.1 vector (Invitrogen). The accuracy of the insert was confirmed by DNA sequencing using miRNA specific primers.

Cell culture and tissue samples from rat/mouse strains.

AML12 (alpha mouse liver 12) cells (a gift from Dr. Rakesh K. Tyagi, Jawaharlal Nehru University, New Delhi, India) and human hepatocellular carcinoma HuH-7 cells (obtained from the National Center for Cell Sciences, Pune, India) were cultured in Dulbecco's modified Eagle's medium with high glucose and Glutamine (HyClone), supplemented with 10% fetal bovine serum (Invitrogen, USA), penicillin G (100 units/mL), and streptomycin sulfate (100 mg/mL) (Invitrogen, USA) in 25 cm^2 tissue culture flasks (NEST, USA) at 37 °C with 5% CO_2.

Wistar female rats at the age of 6 weeks were obtained from the King Institute of Preventive Medicine (Chennai, India). Liver, kidneys, and skeletal muscle were isolated following standard procedures. Liver tissue samples (in RNAlater solution) from male BPH (strain BPH/2J, at inbred generation F66) and BPL (strain BPL/1J, at inbred generation F65) mice at the age of 5 −7 weeks were procured from the Jackson Laboratory (Bar Harbor, ME). Intentionally, young BPH and BPL mice were selected to minimize the effects of age-related confounding factors on gene expression. Likewise, male SHR and WKY liver tissue samples at the age of 4-6 weeks were procured from the Division of Pharmacology, Central Drug Research Institute (Lucknow, India). In addition, liver tissues from male Sprague-Dawley (SD) rats fed with high fat and fructose diet (HFHF) and normal chow-diet fed rats at the age of 32 weeks were also obtained from National Institute of Nutrition (Hyderabad, India). All animal tissue-related procedures were approved by the Institutional Animal Ethics Committee at Indian Institute of Technology Madras (1007/C/06/CPCSEA/IITM/BT/15/NRM-2018;
1007/C/06/CPCSEA/IITM/BT/16/NRM-2018;
1007/C/06/CPCSEA/IITM/BT/19/NRM-2018;
1007/C/06/CPCSEA/IITM/BT/21/NRM-2018)

Transient transfection and reporter assays

AML12 and HuH-7 cells were grown up to 70% confluence in 12-well plates and co-transfected with different doses (125, 250 and 500 ng) of plasmids expressing miR-27a, along with 500 ng/well of m*Hmgcr*-3'UTR-reporter plasmid by lipofectamine(R) 2000 (Invitrogen) according to manufacturer's instructions. Similarly, m*Hmgcr*-3'UTR-reporter wild-type plasmid or m*Hmgcr* 27a mut 3'-UTR construct was co-transfected with miR27a in a dose-dependent manner. In all these co-transfection experiments, the insert-free vector pcDNA3.1 was used as balancing plasmid. After 4 hrs of transfection, the culture media was changed with fresh complete media.

In other co-transfection experiments, AML12 cells were transfected with different doses of Egr1 expression plasmid (obtained from Dr. Wong, (30)) or Egr1 shRNA expression plasmids (obtained from Dr. Xiao, (31)) along with 500 ng/well of the miR-27a pro construct. pcDNA3.1 was used as a balancing plasmid for Egr1 expression plasmid co-transfections while pU6 was used as a control plasmid for the Egr1 shRNA experiments.

In all co-transfection experiments, cells were lysed 36 hrs post-transfection and cell lysates were assayed for luciferase activity as described previously (32,33). Total protein per individual well was also estimated in the same cell lysate by using Bradford reagent (Bio-Rad). The reporter activities were normalized with the total protein content and expressed as luciferase activity/µg of protein or % over control.

RNA extraction and Real-time PCR

Total RNA was extracted from liver tissue samples of BPH and BPL mice or SHR and WKY rats by using Trizol (Invitrogen) as per the manufacturer's instructions. cDNA synthesis was performed using High Capacity cDNA Reverse Transcription Kit (Applied Biosystems) and miR-27a/miR-27b/U6-specific stem-loop (SL) primers (Supplementary Table1). Quantitative Real-time PCR (qPCR) was performed using the DyNAmo HS-SYBR Green qPCR Kit (Finnzymes) and using gene specific primers and a universal reverse primer (Supplementary Table1). The same mmu-miR-27-forward primer was also used to probe for miR-27b expression.

In another set of experiments, total RNA was isolated from AML12 and different tissues (liver, kidney and skeletal muscle) of Wistar rats (mentioned in the "Cell culture and tissue samples from mouse strains" section). Following cDNA synthesis, qPCR was performed using m*Hmgcr* gene specific primers and mouse β-Actin specific primers (Supplementary Table1) as described above. In case of rat samples, qPCR was performed using rat *Hmgcr* gene specific primers and rat β-Actin specific primers (Supplementary Table1).

In certain experiments, AML12 cells were transfected with different doses of miR-27a expression plasmid or 60 nM of locked nucleic acid inhibitor of 27a (LNA 27a) and negative control oligonucleotides (Exiqon, Denmark) by using lipofectamine. Over-expression or down-regulation of miR-27a was determined by qPCR analysis.

In one experiment, for cholesterol depletion, AML12 cells (grown in 12 well plates) were treated with increasing doses (0, 1, 3.6 and 5 mM) of cholesterol-depleting reagent methyl-β-cyclodextrin (HiMedia, India) for 15 minutes. Cholesterol depletion was carried out in serum-free DMEM medium. Following cholesterol depletion, media was changed with fresh serum-free media and the cells were incubated for 6-9 hrs at 37°C in CO_2 incubator.

In another series of experiments, AML12 cells were treated with exogenous cholesterol (20 µg/ml) in serum free media for 6-9 hrs. Next, the cells were processed for RNA isolation followed by qPCR to measure the relative abundance of miR-27a and *Hmgcr* transcript. Total miRNAs isolated from the treated and control cells were subjected to cDNA synthesis followed by qPCR analysis probing for miR-27a and U6 RNA using miR-27a and U6 specific primers.

For hypoxia experiments, AML12 cells were transferred to a desiccator cabinet (Bel-Art, USA) and flushed with argon gas for 2 min and sealed. The cabinet was then placed in an incubator at 37 °C for 12 hours. In parallel, AML12 cells incubated at 37°C in CO_2 incubator for 12 hours were used as a control. RNA isolation In all the qPCR analysis, the relative abundance of miR-27a and *Hmgcr* was determined by calculating $2^{-\Delta\Delta Ct}$ of each reaction (34).

Filipin Staining

AML12 cells were seeded at 60-70% confluency in 12/ 24 well plates overnight at 37 °C with 5% CO_2. The cells were then treated with 20 µg/ml of exogenous cholesterol or 5mM of cholesterol-depleting reagent methyl-β-cyclodextrin (MCD) for 6 hours or 15 min respectively. Post-MCD treatment, the media was changed to serum-free media and the cells were incubated at 37 °C for 6-9 hours. Following treatment with cholesterol or MCD, the cells were washed with PBS and fixed with 3.6% formaldehyde in PBS for 10 min at room temperature.

The fixed cells were washed with PBS and stained with 50 µg/ml of Filipin III (a fluorescent dye that binds to free cholesterol) in the dark at room temperature for 2 hours. Following fixing, the cells were washed with PBS again and imaged using an Olympus U-RFL-T fluorescence microscope (Olympus, Japan).

mRNA stability assays

Actinomycin D, an extensively used and highly specific transcriptional inhibitor, was used to determine the Hmgcr mRNA stability under basal condition as well as upon cholesterol depletion and hypoxia like pathophysiological conditions. In this experiment, AML12 cells were transfected with miR-27 expression plasmid or pcDNA3.1. After 24 hours of transfection, cells were treated with actinomycin D (5 µg/ml) (Himedia, India) for different time points (0, 6, 12 and 24 hours). In both the cases (with/without miR-27a over-expression), Hmgcr mRNA decay was monitored by measuring the *Hmgcr* levels by qPCR as described above. Hmgcr mRNA half-life was determined by using $t_{1/2}$= -t (ln2)/ln(N_t/N_0) as described previously where N_t= mRNA remaining at a specific time t, and N_0= mRNA abundance in the beginning (35). In parallel, the total protein was also isolated at each time point as described below for Western blot analysis. All the experiments were carried out in triplicates. The Hmgcr mRNA half-life from three different experiments was averaged and standard error calculated.

Ago2-Ribonucleoprotein immunoprecipitation (RIP)

To probe the endogenous interaction of miR-27a with *Hmgcr*, Ago2-RIP experiments were carried out as described earlier (36). HuH-7 cells grown at 60% confluence in 100 mm dishes were transfected with 5 µg of miR-27a expression plasmid or pcDNA3 using Targetfect F2 transfection reagent (Targeting Systems, USA). After 24 hrs of transfection, cells were lysed in 100 µl of ice cold polysome lysis buffer [5 mM $MgCl_2$, 100 mM KCl, 10 mM HEPES (pH 7.0) and 0.5% Nonidet P-40] with freshly added 1 mM DTT, 100 U/ml recombinant ribonuclease (Takara, Japan) supplemented with protease

inhibitor cocktail (Sigma Aldrich) by tapping every 5 min for 3 secs over a period of 15min on ice. The lysates were then centrifuged at 14,000 rpm at 4 °C for 10 min. Supernatant was mixed with 900 µl of ice-cold NT2 buffer [50 mM Tris (pH 7.4), 150 mM NaCl, 1 mM $MgCl_2$, 0.05% Nonidet P-40] containing freshly added 200 U/ml recombinant ribonuclease (Takara, Japan), 1 mM DTT, 15 mM EDTA. The lysates were pre-cleared with Rec protein G-Sepharose 4B beads (Invitrogen, USA). Pre-cleared samples were then immunoprecipitated by incubation with 0.75 µg each of anti-Ago2 antibody (abcam, ab57113) and non-immune mouse IgG (Sigma, I5831) was used as a negative control. Incubation was carried out overnight at 4 °C on a rotating platform. On the following day, beads were washed five times with ice-cold NT2 buffer and divided into two fractions—one for RNA isolation to identify miRNA target genes and another for Western blotting to check for successful immunoprecipitation of Ago2. Anti-Ago2 antibody at a dilution of 1:2500 was used for Western blot analysis. RNA was isolated from the other fraction of beads by TRIzol (Invitrogen, USA) followed by purification via Nucleospin miRNA columns (Machery-Nagel, Germany).

Western Blot Analysis

Up-regulation or down-regulation of HMGCR/HIF-1α/Egr1 after transfection experiments/cholesterol treatment/ depletion/hypoxia like pathophysiological condition was determined by Western blotting. Following transfection with miR-27a plasmid or antagomir, AML12 cells were lysed in radioimmunoprecipitation assay buffer [50 mM Tris–HCl (pH 7.2), 150 mM NaCl, 1% (v/v) Triton X-100, 1% (w/v) sodium deoxycholate, 1mM EDTA,and 0.1% (w/v) SDS] supplemented with 1mM PMSF and protease inhibitor cocktail (Sigma, USA). The cell lysates were sonicated for 10-15 sec on ice, followed by centrifugation at 14,000 rpm for 15 minutes at 4˚C, and the supernatant was then collected. The protein concentrations in the cell lysates were estimated by Bradford Assay (Bio-Rad). Equal amount of protein samples (~30-50 µg) per condition were separated by sodium dodecyl sulphate polyacrylamide gel electrophoresis (SDS-PAGE) gel and transferred to activated PVDF membrane (Pall Life Sciences, Mexico). After

blocking with 2-5% of BSA/ non-fat milk for 1 hour at room temperature, the membranes were incubated with specific primary antibody [HMGCR (Abcam, ab174830) at 1:1000 dilution, β-Actin (Sigma, A5441) at 1:7500 dilution, Vinculin (Sigma, V9131),–at 1:7500 dilution, Egr1 (CST, 4153) at 1:1000 dilution] overnight at 4°C. After washing with 1xTBST, the membrane was incubated with HRP-conjugated secondary antibody specific for either rabbit (BioRad # 170-6515 at 1:1500 dilution for HMGCR) or mouse (Jackson Immunoresearch # 115-035-003 at 1:5000 dilution for β-actin and HIF1α) for 1 hr. The protein bands were detected using Clarity™ Western ECL Substrate kit (Bio-Rad) and signal was captured by Chemidoc XRS+ Chemiluminescence Detection system (Bio-Rad). Densitometric analysis of Western blots was performed using Image Lab (Bio-Rad) or NIH Image J software(37).

Chromatin Immunoprecipitation (ChIP) Assays

AML12 cells, seeded in 100 mm dishes at 60-80% confluency, were subjected to hypoxic stress for 12 hours. Following treatment, the cells were cross-linked using formaldehyde at room temperature for 12 min. Next, chromatin was isolated and sheared by sonication followed by a pre-clearing step with Rec protein G-Sepharose 4B beads (Invitrogen, USA). Immunoprecipitation reactions of the pre-cleared samples were carried out by incubation with 5 µg each of ChIP grade antibodies, i.e. anti-Egr1 and pre-immune anti-rabbit IgG (Sigma, I5006) overnight at 4°C. The immunoprecipitated samples were captured by Rec protein G-Sepharose 4B beads, eluted, reverse cross-linked and purified by phenol-chloroform extraction. qPCR was carried out using equal amount of the purified chromatin as template to amplify two different DNA regions harboring Egr1 binding sites in the proximal (~500 bp) promoter domain of miR-27a promoter using two primer pairs (Fig.6) (P1-FP: 5'-TCAAGATAGGCAGGCAAGC-3' and P1-RP: 5'-AGCACAGGGTCAGTTGGAAA-3'; P2-FP: 5'-TTTGTAGGGCTGGGGTAGAG-

3' and P2-RP: 5'-CTGATCCACACCCTAGCCC-3'). Results were expressed as fold enrichment over IgG signal or background.

In silico prediction of miR-27a target genes in the cholesterol biosynthesis pathway

Putative mouse miR-27a target genes were retrieved from TargetScan and miRWalk (Supplementary Table 2). These datasets were used as input for the Panther classification system (http://www.pantherdb.org/) which grouped them based on their molecular functions. Only mapped gene IDs belonging to the cholesterol biosynthesis pathway were selected.

Data presentation and Statistical analysis

All 3'UTR-reporter/promoter-reporter transient transfection experiments were carried out at least three times and results were expressed as mean ± SE of triplicates from representative experiments. Prism 5 program (GraphPad Software, San Diego, CA, USA) was used to determine the level of statistical significance by Student's t-test or one-way ANOVA with Newman-Keuls's post-test, as appropriate.

RESULTS

Comparative genomics analysis of mouse and rat *Hmgcr* gene sequences.

Although mouse models are highly useful to dissect the genetic basis of complex human diseases and various resources are available for genetic mapping in mice (38), most of the quantitative trait loci (QTL) analyses have been performed in rats because of technical difficulties in measuring the cardiovascular phenotypes in mice. We probed the Rat Genome Database (RGD) for elevated lipid or cholesterol QTLs on *Hmgcr*-harboring chromosome 2 within the range of 26000000-28000000 bp and detected six lipid-related QTLs (Fig.1A). The elevated lipid/cholesterol-QTLs and respective LOD [logarithm (base 10) of odds] scores retrieved from RGD are shown in Table 2.

Interestingly, the QTL Stl27 (23837491- 149614623 bp) that harbors *Hmgcr* gene (27480226- 27500654 bp, RGD ID: 2803) displayed the highest linkage (LOD score=4.4) with blood triglyceride levels (Fig.1A). In addition, QTLs- Stl32 (22612952-67612952 bp), Scl55 (26186097- 142053534 bp) also housing the *Hmgcr* locus displayed significant linkage with blood triglyceride levels (LOD score=3.2) and blood cholesterol levels (LOD score=2.83) respectively. Moreover, alignment of the mouse and rat genomic regions at *Hmgcr* locus using mVISTA demonstrated >75% homology between these rodents at exons, introns and untranslated regions (Fig.1B). Interestingly, the extent of homology between each of the twenty *Hmgcr* exons in mouse and rat were, in general, higher (>85%) than the noncoding regions (Fig.1B). Thus, mouse *Hmgcr* appeared as a logical candidate gene for further studies.

Identification of crucial miRNAs involved in differential expression of mouse *Hmgcr* (*Hmgcr*).

To identify the putative miRNA binding sites, we performed an *in silico* analysis of *Hmgcr* 3'-UTR sequence by using multiple bioinformatic algorithms because these programs predict distinct miRNA binding sites (39). Since a lot of differences were observed among the results obtained from these computational algorithms, we selected those miRNAs that were predicted by at least five algorithms. Further, to get a very stringent list of miRNAs, the selected miRNAs were base-paired with *Hmgcr* 3'-UTR to calculate the differences in hybridization free energy indicating the stability of the microRNA-mRNA interaction by two online tools namely PITA and RNAhybrid. In each case, the minimum number of nucleotides in seed sequence was selected as 6 and no mismatch or no G:U wobble base-pairing was allowed in the region of seed sequence. The lower or more negative ΔG (<-10) or $\Delta\Delta G$ (<-20) value predicted by PITA/RNAhybrid represents the stronger binding of the miRNA to the UTR. On following these selection procedures, 7 miRNAs (miR-27a, miR-27b, miR-708, miR-28, miR-351, miR-124 and miR-345) were shortlisted (Table 1). However, only miR-27a and miR-27b were further selected for our studies based on their crucial role in lipid metabolism (40).

In order to validate our *in silico* findings, we probed for Hmgcr and miR-27a/b expression in three rodent models of metabolic syndrome viz. genetically hypertensive blood pressure high (BPH) *vs*. genetically hypotensive blood pressure low (BPL) mice, Spontaneously Hypertensive Rats (SHR) *vs*. Wistar Kyoto (WKY) rats and rats fed with high fructose and fat diet (HFHF) *vs*. rats fed with normal chow diet. Interestingly, Hmgcr protein expression was ~2-fold ($p<0.05$, Fig.S1) higher in BPH liver tissues than BPL. qPCR analysis in the aforementioned tissues demonstrated that the expression of miR-27a and miR-27b significantly differ in liver tissues of BPH and BPL mice. Specifically, the expression of miR-27a was found ~1.45- fold ($p<0.05$, Fig.S1) elevated in BPH tissue than BPL. On the other hand, the expression of miR-27b was ~3-fold ($p<0.05$) higher in BPL tissue than BPH. Likewise, Hmgcr and miR-27a/b levels were also analysed in liver tissues of hypertensive rat models viz. SHR and WKY. Consistently, the Hmgcr protein expression was ~1.6- fold elevated in SHR liver tissues than WKY. Interestingly, miR-27a expression was ~2.5-fold higher in SHR than its normotensive counterpart, WKY ($p<0.05$, Fig.S1). There was no significant change in the mIR-27b levels in SHR and WKY liver tissues. In corroboration, the miR-27a levels were augmented ~4.6-fold ($p<0.05$, Fig.S1) in normal chow-fed rats than High Fat and fructose (HFHF)-fed rats while the Hmgcr levels were ~1.7-fold ($p<0.05$, Fig.S1) diminished in normal chow-fed rats. Taken together, only miR-27a showed an inverse correlation with Hmgcr expression in liver tissues of the aforementioned models indicating it as a promising candidate for functional characterization.

Since the miR-27a binding site is highly conserved across most mammals (Fig.2), we mined the hsa-miR-27a/b expression and *HMGCR* expression in different human tissues using miRmine, DASHR databases and GTEx portal respectively. Interestingly, a significant negative correlation between *HMGCR* expression and miR-27a expression was observed (Fig.2) in both miRmine (Pearson, $r = -0.9007$, $p<0.05$) and DASHR miRNA expression databases (Pearson, $r = -0.8830$, $p<0.05$). On the other hand, miR-27b expression did not show any such inverse correlation with *HMGCR* expression in the same tissues (Fig.S5).

miR-27a negatively regulates Hmgcr protein levels.

In light of *in silico* analysis, we probed the role of miR-27a in *Hmgcr* gene regulation. Watson-Crick base pairing between miR-27a and *Hmgcr* 3'-UTR (generated by miRanda) revealed that the 2-7 base seed sequence of miR-27a has perfect complementarity to its putative binding site present in the m*Hmgcr* 3'-UTR (Fig.2A). First, we examined the relation between the expression of miR-27a and *Hmgcr* transcripts in cultured AML-12, N2a cells as well as rat liver, kidney and skeletal muscle tissues. Interestingly, miR-27a showed a significant negative correlation with *Hmgcr* expression in the aforementioned samples (Pearson, r = - 0.9550, Fig.2C). To examine whether miR-27a targets *Hmgcr*, pre-miRNA plasmid expressing miR-27a, was co-transfected with the m*Hmgcr* 3'-UTR/luciferase reporter construct into mouse AML12 and human HuH-7 cells (Fig.3A, B); Indeed, over-expression of miR-27a caused a dose-dependent reduction in the m*Hmgcr* 3'UTR reporter activity in both AML12 (one-way ANOVA F=10.95, up to ~85%, p<0.0001) and HuH-7 cells (one-way ANOVA F=7.31, up to ~ 34%, p<0.001) (up to ~5.0-fold, p<0.001) as wells as endogenous HMGCR protein level (Fig.3E, F). Further, our qPCR analysis showed that over-expression of pre-miR27a led to a dose-dependent increase in the expression of the mature form of miR-27a in AML12 (one-way ANOVA F=10.48,~ up to 1770%, p<0.01) and HuH-7 (one-way ANOVA F=4.66, up to ~ 125%, p<0.05) cells (Fig.3C and D). Consistently, the m*Hmgcr* 27a mut 3'-UTR construct (devoid of miR-27a binding site) showed no significant reduction in the m*Hmgcr*-3'UTR reporter activity (Fig.3A, B).

Moreover, to test the specificity of interactions of miR-27a with *Hmcgr* 3'-UTR, we carried out co-transfection experiments with miR-764 which does not have binding sites in the 3'-UTR region (Fig.S2). Furthermore, transfection of locked nucleic acid inhibitor of 27a (LNA 27a) in AML12 cells led to enhancement of Hmcgr mRNA (~3.8-fold, p<0.05) and protein levels (~1.4-fold, p<0.05) (Fig.4B, C). In corroboration, RIP assays with antibody against Ago2, an integral component of RISC complex, showed (~5 fold) enrichment of *HMGCR* in the Ago2-immunoprecipitated RNA fraction of HuH-7 cells over-expressing miR-27a thereby confirming the direct interaction of miR-27a with the *Hmgcr* 3'-UTR (Fig.4D). Despite the binding site of miR-27b, co-transfection of

different doses of miR-27b expression plasmid did not cause significant decrease in m*Hmgcr*-3'UTR reporter activity (Fig.S7).

Role of cholesterol in miR-27a-mediated regulation of Hmgcr.

To determine whether modulation in endogenous cholesterol level affects the post-transcriptional regulation of *Hmgcr*, AML12 cells were treated with exogenous cholesterol or methyl-β-cyclodextrin (MCD), a well known cyclic oligosaccharide that is widely used to reduce intracellular cholesterol levels (41). Indeed, cholesterol treatment showed ~1.9-fold ($p<0.05$) enhancement of miR-27a levels (Fig.5A) and diminished Hmgcr protein levels (Fig.5C). In concordance, cholesterol depletion by MCD caused a ~3-fold ($p<0.05$) reduction in the endogenous expression of miR-27a (Fig.5D) and augmented Hmgcr protein levels (Fig.5F). Further, RIP assays using anti-Ago2 antibody in cholesterol-treated HuH-7 cells revealed significant enrichment of *HMGCR* (~2.2-fold, $p<0.01$) (Fig.7C) and miR-27a levels (~1.7-fold, $p<0.001$) (Fig.7D) suggesting *in vivo* interaction of *HMGCR* with miR-27a under elevated cholesterol conditions. No significant difference was observed in *HMGCR* levels in the RNA fraction immunoprecipitated using pre-immune anti-mouse IgG antibody on miR-27a over-expression (Fig.S8).

Role of Egr1 in miR-27a expression.

To understand the possible mechanism of regulation of miR-27a we predicted the putative transcription factor binding sites on the proximal miR-27a promoter domain (~500 bp) using two independent programs: LASAGNA and JASPAR (Supplementary Table 2). Egr (early growth response) 1, a zinc finger transcription factor predominantly expressed in the liver, plays a crucial role in the transcriptional regulation of most cholesterol biosynthesis genes including *Hmgcr* (42). These programs revealed six Egr1 binding sites in the selected region of miR-27a promoter domain as shown in Fig.6A.

Next, we validated the role of Egr1 in the activation of miR-27a promoter upon over-expression and down-regulation of Egr1. pcDNA3.1 and pU6 were used as balancing plasmids for Egr1 and Egr1 shRNA expression plasmid co-transfections respectively. Over-expression of Egr1 caused a ~3-fold enhancement of miR-27a

promoter activity (one-way ANOVA F=36.41, p<0.0001) (Fig.6B). A concomitant increase in the endogenous miR-27a levels upon Egr1 over-expression was also observed (~4-fold, p<0.05) (Fig.6D). In corroboration, co-transfection of Egr1 shRNA expression plasmid resulted in a ~2.2-fold reduction in the miR-27a promoter activity (one-way ANOVA F=6.955, p<0.05) (Fig.6C). Likewise, Egr1 down-regulation diminished endogenous miR-27a levels (~2-fold, p<0.05) (Fig.6E). Thus, Egr1 plays a crucial role in the transcriptional activation of miR-27a.

Intracellular cholesterol modulates miR-27a expression via Egr1

As Egr1 activates miR-27a promoter and cholesterol modulates miR-27a expression, we sought to test the effect of intracellular cholesterol modulation on Egr1 expression. Indeed, Western blot analysis revealed that exogenous cholesterol treatment caused Egr1 augmentation (~4.5-fold) (Fig7A) while cholesterol depletion resulted in diminished (~1.8-fold) Egr1 levels (Fig7B). Next, to test whether there is enhanced interaction of miR-27a and *Hmgcr* 3'-UTR *in vivo* under elevated cholesterol conditions, RIP assays using anti-Ago2 and anti-IgG antibodies were performed in HuH-7 cells. Elevated cholesterol levels in the cells caused a significant (~2.2-fold) enrichment of *HMGCR* (~2.2-fold, p<0.01) compared to control (Fig.7C). Likewise, the miR-27a levels in the Ago2-immunoprecipitated fraction showed a ~1.72-fold higher enrichment as compared to the untreated cells (Fig.7D). RNA immunoprecipitated using pre-immune anti-mouse IgG antibody showed no significant difference in miR-27a and *HMGCR* levels between treated and untreated conditions (Fig.S8).

Effect of hypoxia stress on miR-27a-mediated *Hmgcr* regulation: Involvement of Egr1.

Since hypoxia (oxygen deprivation) impairs cholesterol metabolism (an oxygen-dependent process) by stimulating the HMGCR degradation (22,43), we tested whether miR-27a regulates the *Hmgcr* expression under such pathophysiological conditions. AML12 cells subjected to hypoxia for 12 hours showed ~1.4-fold (p<0.05) higher miR-27a expression than basal condition (Fig.8A). This observation is consistent with previous reports documenting the activation of miR-27a in various cell types (44-47).

Indeed, Western blot analysis revealed over-expression of HIF-1α, Egr1 and down-regulation of Hmgcr during these experiments (Fig.8B).

Next, ChIP assays were carried out to probe for the interaction of Egr1 with miR-27a promoter during hypoxia (Fig.8D). At the basal level, anti-Egr1 antibody resulted in significant amounts of immunoprecipitation of miR-27a promoter domain when P2 primer pair (mentioned in the materials and methods section) was used for qPCR analysis (Student's *t*-test, ~2.5-fold, $p<0.001$); on the other hand, in hypoxia-treated AML12 cells, the anti-Egr1 antibody showed even more pronounced enrichment of miR-27a promoter domain amplified by primer pair P2 (one-way ANOVA $F=22.33$, $p<0.001$). No significant difference in the fold-enrichment over IgG was observed using Egr1 antibody immunoprecipitated chromatin in basal and hypoxia condition for primer pair P1 (Fig.S9) suggesting that Egr1 sites in the region amplified by these primers (Egr1 cluster 1) are non-functional. This is reminiscent of a previous study where hypoxia alters miR-27a expression in human pulmonary artery endothelial cells (HPAECs) via Egr1 (46).

miR-27a represses Hmgcr by post-translational inhibition.

miRNAs act on their mRNA targets either by triggering mRNA degradation or translational repression. In order to unfold the mechanism of action of miR-27a on *Hmgcr*, mRNA stability assays using actinomycin D were carried out in AML12 cells over-expressing miR-27a (Fig.9). Hmgcr mRNA at different time points of actinomycin incubation were analysed by qPCR in AML12 over-expressing miR-27a or control (without miR-27a transfection). Interestingly, no change in the Hmgcr mRNA half-life was observed on ectopic over-expression of miR-27a (Fig.9A, B). However, the Hmgcr protein levels showed a time-dependent reduction following actinomycin D treatment in AML12 cells transfected with miR-27a (Fig.9C) suggesting that translational control is the predominant step in miR-27a-mediated Hmgcr regulation.

DISCUSSION

Overview

Presently, statins are widely used for the treatment of hypercholesterolemia and to lower the risk of cardiovascular complications. However, statins have altered efficacies in patients as well as well-established adverse effects including myalgias, muscle or gastrointestinal cramps and other symptoms (48). The safety and efficacy concerns over the long-term use of statins to treat elevated cholesterol levels call for alternative therapeutic interventions for lowering plasma lipids. The emerging role of miRNAs as crucial regulators of lipid metabolism has been documented and well-reviewed (49). As such, they serve as promising candidates for miRNA-based therapeutics. Moreover, owing to their short sequence and conservation across most vertebrates, miRNAs are easy therapeutic targets and the same miRNA-modulating compound can be used both for the pre-clinical studies and in clinical trials (50). Despite several studies highlighting the association between the SNPs present in the *HMGCR* locus and different cardiovascular disease states including dyslipidemia, myocardial infarction, stroke and elevated blood pressure (11,51), the role of miRNAs in its regulation is only partially understood. In this study, we undertook a systematic approach to identify the key miRNAs that may regulate mouse *Hmgcr* gene expression under basal as well as pathophysiological conditions. Our extensive computational analysis using multiple bioinformatic algorithms coupled with experimental analysis (miR-27a over-expression/downregulation experiments along with Ago2-RIP assays) identified miR-27a as a key regulator of *Hmgcr* expression (Figs. 3 and 4). Of note, these findings are in concordance with a previous study reporting the repression of *HMGCR* 3'-UTR luciferase activity in HuH-7 cells transfected with miR-27 mimics (52).

Regulation of Hmgcr expression by miR-27a is conserved across various mammalian species.

Alignment of *Hmgcr*-3'UTR sequence of various mammalian species harboring the miR-27a binding site (human, rat, hedgehog, rabbit, chimpanzee, cow, rhesus, shrew, dog, cat, armadilo, elephant and opossum) showed that the miR-27a binding site is

significantly conserved across the mammalian species (Fig.2). This conservation enables us to assess the physiological effect of over-expression or down-regulation of miR-27a in model organisms before human studies. We selected three rodent models of metabolic syndrome to validate our *in silico* predictions viz. BPH *vs*. BPL mice, SHR *vs*. WKY rats and rats fed with high fructose and fat diet (HFHF) *vs*. rats fed with normal chow diet; all these models show altered serum lipid profiles as compared to their controls indicating deregulation of cholesterol homeostasis [(Mouse Phenome Database, Jackson Laboratory; www.jax.org/phenome, The Rat Genome Database (RGD); http://rgd.mcw.edu and (53)]. Interestingly, miR-27a expression in liver tissues showed an inverse correlation with Hmgcr levels in all these models (Fig.S1) while miR-27b levels were not negatively correlated to Hmgcr expression (Fig.S5). Moreover, miR-27a also showed a significant negative correlation with *Hmgcr* expression in cultured AML12 cells and mouse neuroblastoma N2a cells as well as rat liver, kidney and skeletal muscle tissues (Fig.2) highlighting it as a promising candidate for further cellular and molecular studies.

miR-27a regulates Hmgcr expression by translational repression.

miRNAs silence their targets by either translational repression or mRNA degradation. Generally, miRNAs exert their action by translational inhibition followed by mRNA deadenylation, decapping and decay (54). Of late, accumulating evidence suggests that miRNA-mediated mRNA repression can be seen even without the necessity of transcript degradation (55-57). In order to decipher the exact mode of action of miR-27a, mRNA stability assays were performed in AML12 cells over-expressing miR-27a. After 24 hours of miR-27a transfection, transcription was attenuated and mRNA/protein levels were monitored at different time points following transcriptional inhibition. qPCR analysis suggest that the Hmgcr mRNA half-life did not change significantly when the cells were transfected with miR-27a (Fig.9). In corroboration, over-expression of miR-27a in AML12 cells also did not alter the steady state Hmgcr mRNA levels (Fig.S4). On the other hand, the Hmgcr protein levels diminished drastically in a time-dependent manner suggesting that translational control is the pre-dominant event of miR-27a-mediated Hmgcr repression (Fig.9C).

Mechanism of regulation of miR-27a: crucial role of Egr1

In view of the key role of miR-27a in regulating Hmgcr we sought to unravel how miR-27a might be regulated under basal and pathophysiological conditions. A series of computational and experimental analyses suggested, for the first time to our knowledge, a crucial role of Egr1 in the activation of miR-27a expression. Egr1, a zinc finger transcription factor belonging to the early growth response gene family, binds to a GC-rich consensus region, GCG(T/G)GGGGG (58) and influences a variety of target genes involved in physiological stress response, cell metabolism, proliferation and inflammation (59). Egr1 has also been implicated in various cardiovascular pathological processes including atherosclerosis, cardiac hypertrophy and angiogenesis (60). Among the Egr family of genes, Egr1 is pre-dominantly expressed in the liver as well as liver-derived cell lines and targets multiple cholesterol biosynthesis genes (42,61). In light of computational prediction of multiple Egr1 binding sites in the proximal miR-27a promoter domain (Fig.6A), we investigated the role of Egr1 in miR-27a expression. Indeed, over-expression/down-regulation of Egr1 resulted in enhanced/diminished miR-27a promoter activity in AML12 cells (Fig.6B, C). Consistent with the computational predictions, ChIP analyses confirmed the *in vivo* interaction of Egr1 with the miR-27a promoter (Fig.8D). This is in corroboration with a previous study that reported Egr1 down-regulation attenuates miR-27a expression in human pulmonary artery endothelial cells (46).

miR-27a also targets multiple genes in the cholesterol biosynthesis pathway.

miR-27a, an intergenic miRNA, is transcribed from the miR-23a-miR-27a-miR-24 cluster located on chromosome 8 in mice. Interestingly, dysregulation of miR-27a has been associated with several cardiovascular phenotypes including impaired left ventricular contractility, hypertrophic cardiomyopathy, adipose hypertrophy and hyperplasia (62). miR-27a regulates several genes including involved in adipogenesis and lipid metabolism including Retinoid X receptor alpha (RXRα), ATP-binding cassette transporter (ABCA1) also known as the cholesterol efflux regulatory protein, fatty acid synthase (FASN), sterol regulatory element-binding proteins (SREBP-1 and -2), peroxisome proliferator-activated receptor (PPAR-α and -γ), Apolipoprotein A-1,

Apolipoprotein B-100 and Apolipoprotein E-3 [as reviewed in (40)]. hsa-miR-27a-3p is expressed in multiple tissues with pronounced expression in the liver, breast and testis (Fig.S2B). Interestingly, TargetScan and miRWalk predictions coupled with Panther pathway analysis revealed five additional cholesterol biosynthesis-related gene targets: 3-Hydroxy-3-Methylglutaryl-CoA synthase 1 (*Hmgcs1*), Mevalonate kinase (*Mvk*), Isopentyl-diphosphate delta isomerase 2 (*Idi*2), Geranylgeranyl pyrophosphate synthase (*Ggps*1) and Squalene synthase (*SS*) indicating that miR-27a might regulate the multiple genes in the cholesterol biosynthesis pathway (Fig.10). This is reminiscent of miR-27a/b target prediction documented in a recent review (63). Indeed, our *in vitro* experiments revealed miR-27a also targets Mevalonate kinase (*Mvk*) and Squalene synthase (*SS*) in AML12 cells (Supplementary Table 3).

Pathophysiological implications of Hmgcr regulation by miR-27a.

HMGCR is tightly regulated by sterols at multiple levels by transcriptional, post-transcriptional and post-translational mechanisms (as reviewed in (64,65)). In brief, elevated sterols diminish *HMGCR* expression by inhibition of Sterol Regulatory Element Binding Protein 2 (SREBP-2) transcription factor (66,67). The post-transcriptional and post-translational regulatory systems operate independent of SREBP pathway and form an important aspect of sterol-mediated HMGCR regulation. Post-translational regulation is executed by sterol or non-sterol intermediates via INSIG dependent ER-associated protein degradation (ERAD) mechanism involving ubiquitin-proteosomal degradation of HMGCR (67,68). However, the effect of elevated sterols on miRNA-mediated regulation of *HMCGR* is partially understood. In the view of crucial role of sterols in HMCGR regulation, we asked whether enhanced cholesterol levels modulate endogenous miR-27a levels? Indeed, exogenous cholesterol treatment to AML12 cells enhanced miR-27a levels as well as diminished Hmgcr protein levels (Fig.5). In order to rule out the possibility that this repression in Hmgcr protein levels is solely because of INSIG-mediated ERAD mechanism, we performed RIP assays in AML12 cells treated with cholesterol. Our RIP assays using anti-Ago2 antibodies further confirmed the direct interaction of miR-27a with *Hmgcr* suggesting that post-transcriptional regulation of Hmgcr by miR-27a is an additional mechanism for down-regulation of Hmgcr levels

under high cholesterol conditions. Moreover, qPCR analyses in liver tissues of rats fed with a high fructose and high fat diet indicate altered miR-27a expression (Fig.S1). This is reminiscent of multiple studies showing modulation of miR-27a expression in rodents fed with a high-fat diet (69,70). Of note, circulating levels of miR-27a were also diminished in subjects with hypercholesterolemia or hypertension (71). Thus, this study revealed the crucial role of intracellular cholesterol on Hmgcr expression via miR-27a.

Hypoxia, a manifestation of liver damage, has been associated with cardiovascular disease pathophysiology (72). Moreover, hypoxia contributes to hepatic lipid accumulation thereby causing dysregulation of lipid metabolism and hyperlipidemia (73,74). The regulation of HMGCR in response to hypoxia by Hypoxia-inducible Factor (HIF) family of proteins has been well- studied (22,73). However, the role of miRNAs in the post-transcriptional regulation of *Hmgcr* under hypoxia is not understood. Interestingly, our results are in corroboration of previous studies indicating that hypoxia stimulates miR-27a expression (44-47). Is the binding of Egr1 to miR-27a promoter altered under hypoxic stress? Indeed, our ChIP-qPCR analysis revealed enhanced binding of Egr1 with miR-27a promoter (Fig.8). Interestingly, Western blot analysis revealed that hypoxia augmented Egr1 levels in AML12 cells while lowering Hmgcr levels (Fig.8). This is in corroboration with multiple studies showing elevated Egr1 levels during hypoxia (75,76).

Conclusions and perspectives.

In conclusion, this study identified miR-27a as crucial regulator of *Hmgcr* as well as several other genes in the cholesterol biosynthesis pathway. In addition, miR-27a regulated Hmgcr expression under elevated cholesterol / hypoxic stress conditions via Egr1. Thus, this study provides new insights on the plausible role of miR-27a in the post-transcriptional regulation of Hmgcr thereby implicating its role in cholesterol homeostasis under pathophysiological conditions.

In the view of miR-27a targeting several crucial genes in the cholesterol biosynthesis pathway, miR-27a mimic can be used as an effective therapeutic intervention to treat hypercholesterolemia/dyslipidemia. Indeed, administration of miR-27a mimics in apolipoproteinE knockout (apoE KO) mice resulted in diminished lipid

levels in both plasma and peritoneal macrophages (77). Our findings and other studies provide strong impetus for further preclinical studies and subsequent human trials for miR-27a as a novel lipid-lowering agent.

Table 1: A list of predicted miRNAs having potential binding sites in the 3'-UTR of m*Hmgcr*

miRNA	Number of Prediction Programs	Seed Sequence (Number of bases)	ΔΔG Calculated by PITA	ΔG Calculated by RNA HYBRID (Kcal/mol)
mmu-miR-124	5	7	-10.62	-29.5
mmu-miR-28	5	8	-10.28	-22.2
mmu-miR-345-5p	5	8	-11.08	-32
mmu-miR-351	5	8	-16.89	-33.6
mmu-miR-708	5	7	-14.34	-27.4
mmu-miR-27a	5	6	-10.13	-20.7
mmu-miR-27b	5	6	-10.74	-22.6

Table 2 Genomic position and LOD score of various lipid/cholesterol QTLs present on rat chromosome 2 (26000000- 28000000 bp)*

Blood Pressure QTLs	Start position (bp)	Stop position (bp)	LOD Score
Stl32	22612952	67612952	3.2
Stl27	23837491	149614623	4.4
Scl55	26186097	142053534	2.83
Sffal3	27760301	72760301	6.78
Scl17	228712271	266435125	3.4
Scl8	231621666	266435125	4.4

*This data was retrieved from Rat genome database (http://rgd.mcw.edu/rgdweb/search/qtls.html?100).

FIGURE LEGENDS

Fig.1. Graphical representation of rat elevated lipid/cholesterol-QTLs and homology between mouse- and rat-*Hmgcr* gene sequences. (A)The lipid/cholesterol-QTLs and their respective LOD scores (retrieved from Rat Genome Database) were plotted. The genomic position of rat *Hmgcr* gene is indicated. (B) Conservation analysis of rat and mouse *Hmgcr* sequences was performed using mVISTA. The horizontal axis represents the rat *Hmgcr* gene (chr2: 27480226-27500654) as the reference sequence, whereas the vertical axis indicates the percentage homology between rat and mouse *Hmgcr* gene (chr13: 96,650,579-96,666,685). Here, window size (length of comparison) was set to 100 bp with a minimum of 70% match. The annotation of gene is represented by different colors. Both the mouse and rat *Hmgcr* genes comprise of twenty exons; 5'-UTR is not visible in the homology plot due to their very small sizes. CNS: conserved non-coding sequences; UTR: Untranslated region.

Fig.2 miR-27a binding sites in the 3'-UTR of *Hmgcr* and inverse correlation of mmu-miR-27a-3p/hsa-miR-27a-3p and *Hmgcr/HMGCR* expression. (A) Schematic representation of the *Hmgcr* gene showing the miR-27a binding site in the 3'-UTR. The complementarity between the seed region of miR-27a and mHmgcr-3'UTR is depicted in bold and capital. Positions of the transcription initiation/cap site (indicated as +1 bp), 5'-UTR, exons and 3'-UTR are also shown. **(B)** The conservation of the miR-27a binding site in the 3'-UTR of *Hmgcr* across different mammals. The seed region along with the mature mmu-miR-27a sequence is also shown at the top of the figure. **(C)** Negative correlation between *Hmgcr* mRNA and miR-27a expression in cultured AML-12 cells as well as rat liver, kidney and skeletal muscle tissues**.** Wistar female rats at the

age of 6 weeks were procured following institutional norms. RNA and miRNAs isolated from AML12 cells and the aforementioned tissues were probed for *Hmgcr* and miR-27a expression by qPCR. *Hmgcr* mRNA and miR-27a expressions were normalized to mouse β-actin mRNA and U6 RNA in the same sample respectively. A strong inverse correlation was observed and the Pearson r and p values are indicated.

(D) Inverse correlation between *HMGCR* and hsa-miR-27a-3p expression in different tissues. Endogenous *HMGCR* expression profiles in different human tissues was obtained from the GTEx portal while hsa-miR-27a-3p expression data was retrieved from miRmine and DASHR respectively as detailed in the materials and methods. Only tissues common to the GTEx portal and DASHR or miRmine were chosen for correlation analysis and the expression is represented as fold change (when normalized to pancreas for miRmine and spleen for DASHR). The Pearson r and p values for each database are shown.

Fig.3: miR-27a negatively regulates Hmgcr in AML12 and HuH-7 cells. (A and B) Down-regulation of Hmgcr 3'-UTR/luciferase activity by miR-27a. The mHmgcr-3'UTR reporter construct was co-transfected with increasing doses of miR-27a expression plasmid in (A) AML12, (B) HuH-7 cells and luciferase activity was assayed. Values were normalized to total protein and are mean ± SE of triplicate values. Statistical significance was determined by one-way ANOVA with Newman-Keuls multiple comparison test. *, ** and *** indicate $p<0.05$, $p<0.01$ and $p<0.001$ respectively as compared to the control (without miRNA-27a over-expression). (C and D) Transfection of miR-27a expression plasmid results in over-expression of miR-27a in AML12 and HuH-7 cells respectively. AML12 or HuH-7 cells were transfected with increasing doses of miR-27a expression plasmid followed by total RNA isolation and cDNA synthesis. The expression of miR-27a was analyzed by qPCR using miRNA specific primers and miR-27 expression as normalized to U6 RNA. Statistical significance was determined by one-way ANOVA with Newman-Keuls multiple comparison test. * and ** indicate $p<0.05$ and $p<0.01$ respectively as compared to the control (without miRNA-27a over-expression). (E and F) Down-regulation of Hmgcr/HMGCR was confirmed by Western blot analysis and shown in the lower panel.

Fig.4: Specific interaction of miR-27a with Hmgcr 3'- UTR. (A and B) The relative expressions of miR-27a and *Hmgcr* upon transfection of 60 nM of locked nucleic acid inhibitor of 27a (LNA27a) or control oligos in AML12 cells were determined by qPCR using miRNA/gene-specific primers. miR-27a and *Hmgcr* expressions were normalized to U6 RNA and mouse β-actin mRNA in the same sample respectively. Statistical significance was determined by Student's *t*-test (unpaired, 2-tailed). * indicates $p<0.05$ as compared to the control (i.e., when transfected with control oligos). (C) Representative Western blot analysis of Hmgcr protein levels in AML12 cells upon transfection of 60 nM of LNA 27a or control oligos. The Hmgcr protein levels are normalized to vinculin and indicated below the blots. Normalized values are shown as mean ± SE from triplicate wells. (D) Ribonucleoprotein Ago2 precipitation analysis in HuH-7 cells over-expressing miR-27a. HuH-7 cells were transfected with miR-27a expression plasmid. HuH-7 cells transfected with pcDNA3.1 were used as control. After 30-36 hours of transfection, miRNA-27-RISC complexes were immunoprecipitated with Ago2/ pre-immune anti-mouse IgG antibody and *HMGCR* levels were measured by qPCR using h*Hmgcr* (*HMGCR*) primers (Supplementary Table1). The *HMGCR* expression was normalized to the corresponding input in each condition; expressed as % input and is mean ± SE for quadruplets. Statistical significance was determined by Student's *t*-test (unpaired, 2-tailed). ** indicates $p<0.01$ as compared to the control (co-transfected with pcDNA 3.1). (E) Immunoprecipitation of Ago2 was confirmed by Western blotting. Ago2 was pulled down when appropriate antibody was used (lanes 5 and 6) while the mouse IgG revealed no immunoprecipitation of Ago2 (lanes 3 and 4).

Fig. 5: Intracellular cholesterol modulates the expression of miR-27a in AML12 cells. AML12 cells were treated with increasing doses of cholesterol ((3β)-cholest-5-en-3-ol) or cholesterol-depleting reagent methyl-β-cyclodextrin (MCD) for 6 hours or 15 minutes respectively. After incubation for 6-9 hrs in serum free media, the cells were processed for RNA, protein isolation and fluorescence microscopy. (A and D) miR-27a levels were determined by qPCR on exogenous cholesterol (20 µg/ml) or MCD (5 mM) treatment in AML12 cells respectively. The miR-27a expression was normalized to U6

RNA and indicated as mean ± SE for triplicate values. Statistical significance was determined by Student's *t*-test (unpaired, 2-tailed). * $p<0.05$ as compared to the control condition. The cholesterol/MCD treatments in AML12 cells were confirmed by staining intracellular cholesterol using Filipin stain followed by fluorescence microscopy (B and E). (C and F) Western blot analysis of total protein isolated from AML12 cells treated with cholesterol/MCD was carried out for Hmgcr and β-actin levels.

Fig. 6. Role of Egr1 in miR-27a expression. (A) Schematic representation of the proximal (~ 1 kb) mmu-miR-27a promoter domain harboring the Egr1 binding sites as predicted by LASAGNA tool and JASPAR . (B and C) Effect of over-expression/down-regulation of Egr1 on miR-27a expression. AML 12 cells were co-transfected with increasing doses of (B) Egr1 expression plasmid or (C) Egr1 shRNA expression plasmid and mmu-miR-27a promoter construct. pcDNA3.1and pU6 were used as balancing plasmids respectively. Results are expressed as mean ± SE for triplicate values. Statistical significance was determined by one-way ANOVA with Newman-Keuls multiple comparison test. * and **** indicate $p<0.05$ and $p<0.0001$ respectively as compared to the basal mmu-miR-27a promoter activity. Over-expression/down-regulation of Egr1 was confirmed by Western blot analysis. AML12 cells were co-transfected with mmu-miR-27a promoter and 500 ng of (D) Egr1 expression plasmid or (E) Egr1 shRNA expression plasmid followed qPCR to probe for the endogenous levels of miR-27a (normalized to U6 RNA). Statistical significance was determined by Student's *t*-test (unpaired, 2-tailed). * $p<0.05$ as compared to the control condition (transfected with only pcDNA 3.1 or pU6 plasmid respectively).

Fig. 7. Effect of intracellular cholesterol on Egr1 and interaction of miR-27a with the Hmgcr 3'-UTR. AML12 cells were treated with (A) 20 μg/ml of cholesterol [(3β)-cholest-5-en-3-ol]or (B) 5 mM of cholesterol-depleting reagent methyl-β-cyclodextrin (MCD) for 6 hours or 15 minutes respectively and Western blot analysis of total proteins was carried out probing for Egr1 and vinculin. Relative levels of Egr1 after normalization with vinculin are shown. (C and D) Enrichment of *HMGCR* and miR-27a in Ago2-IP RNA of HuH-7 cells treated with exogenous cholesterol. HuH-7 cells were treated with

20 µg/ml of cholesterol [(3β)-cholest-5-en-3-ol] for 6 hours and the total RNA fraction from the Ago2/IgG-IP samples (in basal and cholesterol treated cells) was subjected to qPCR using (C) *HMGCR* and (D) miR-27a primers. The *HMGCR*/miR-27a expression was normalized to the corresponding input in each condition and represented as % input. Statistical significance was determined by Student's *t*-test (unpaired, 2-tailed). ** p<0.01 and ***p<0.001 as compared to the basal condition.

Fig. 8. Effect of hypoxia on miR-27a-mediated regulation of *Hmgcr*. (A) Effect of hypoxic stress on miR-27a expression. AML12 cells were subjected to hypoxic stress for 12 hours and endogenous miR-27a levels were analysed by qPCR analysis. Statistical significance was determined by Student's *t*-test (unpaired, 2-tailed). * p<0.05 as compared to the basal condition. (B) Effect of hypoxia on Egr1 expression. AML12 cells were subjected to hypoxia for 12 hours and Western blot analysis was performed to probe for Hmgcr, HIF-1α, vinculin and β-actin. (C) Pictorial representation of proximal (~ 500 bp) mmu-miR-27a promoter domain harboring two clusters of the Egr1 binding sites. (D) Effect of hypoxic stress on binding of Egr1 with miR-27a promoter domain. ChIP assay was carried out with chromatin isolated from AML12 cells treated with/without exposure to hypoxia. qPCR was performed with DNA purified from respective cocktails using primer pair P2 amplifying 140 bp DNA segment (Egr1 cluster 2) in the proximal miR-27a promoter domain. Statistical significance was determined by Student's *t*-test (unpaired, 2-tailed) and one-way ANOVA with Newman-Keuls multiple comparison test. $$p<0.05 as compared to basal IgG condition (Student's *t*-test). ***p<0.001 as compared to IgG fold enrichment under hypoxia (one-way ANOVA).

Fig.9. miR-27a regulates *Hmgcr* expression by translational repression. AML12 cells were transfected with 500 ng of miR-27a expression plasmid or pcDNA3.1 (as control). After 24 hours of transfection, they were incubated with actinomycin D (5 µg/ml) for different time points. (A) Hmgcr mRNA levels were plotted relative to 0 hour time point as described in the materials and methods section and results are expressed as mean ± SE of three independent experiments. (B) Endogenous Hmgcr mRNA half-life estimation in AML12 cells on ectopic over-expression of miR-27a. The mRNA half-

life of *Hmgcr* was measured over 24 hours in the presence of 5 µg/ml of actinomycin D in both miR-27a co-transfected AML12 cells and control cells (.i.e., AML12 cells transfected with pcDNA3.1). Hmgcr mRNA half-life is represented as mean ± SE of three independent experiments. No significant change in Hmgcr mRNA half-life was observed on ectopic over-expression of miR-27a (C) Effect of miR-27a over-expression on Hmgcr protein levels. AML12 cells transfected with either miR-27a expression plasmid or pcDNA 3.1 and incubated with actinomycin D for different time points. Western blot analysis of total proteins was carried out probing for Hmgcr and vinculin. (C) The relative Hmgcr protein levels normalized to vinculin for different time points are also shown. (D) The Hmgcr levels in miR-27a over-expressed AML12 cells were normalized to those in the corresponding control condition for each time point and plotted against time.

Fig.10. Putative and validated targets of miR-27a in the cholesterol biosynthesis pathway. miR-27a gene targets predicted by *in silico* tools viz. miRWalk and TargetScan were categorized based on their molecular functions and only gene targets mapped to the cholesterol biosynthesis pathway are shown. The solid line represents validated targets (this study) while the dotted line represents predicted miR-27a gene targets in the pathway.

REFERENCES

1. Benjamin, E. J., Virani, S. S., Callaway, C. W., Chamberlain, A. M., Chang, A. R., Cheng, S., Chiuve, S. E., Cushman, M., Delling, F. N., Deo, R., de Ferranti, S. D., Ferguson, J. F., Fornage, M., Gillespie, C., Isasi, C. R., Jimenez, M. C., Jordan, L. C., Judd, S. E., Lackland, D., Lichtman, J. H., Lisabeth, L., Liu, S. M., Longenecker, C. T., Lutsey, P. L., Mackey, J. S., Matchar, D. B., Matsushita, K., Mussolino, M. E., Nasir, K., O'Flaherty, M., Palaniappan, L. P., Pandey, A., Pandey, D. K., Reeves, M. J., Ritchey, M. D., Rodriguez, C. J., Roth, G. A., Rosamond, W. D., Sampson, U. K. A., Satou, G. M., Shah, S. H., Spartano, N. L., Tirschwell, D. L., Tsao, C. W., Voeks, J. H., Willey, J. Z., Wilkins, J. T., Wu, J. H. Y., Alger, H. M., Wong, S. S., Muntner, P., and Epidemi, A. H. A. C. (2018) *Circulation* **137**, E67-E492
2. Sathiyakumar, V., Kapoor, K., Jones, S. R., Banach, M., Martin, S. S., and Toth, P. P. (2018) *Trends Pharmacol Sci*
3. Palacio Rojas, M., Prieto, C., Bermúdez, V., Garicano, C., Núñez Nava, T., Martínez, M., Salazar, J., Rojas, E., Pérez, A., Marca Vicuña, P., González Martínez, N., Maldonado Parra, S., Hoedebecke, K., D?Addosio, R., Cano, C., and Rojas, J. (2017) *F1000Research* **6**
4. Athyros, V. G., Doumas, M., Imprialos, K. P., Stavropoulos, K., Georgianou, E., Katsimardou, A., and Karagiannis, A. (2018) *Hormones* **17**, 61-67
5. Geelen, M. J. H., Gibson, D. M., and Rodwell, V. W. (1986) *Febs Letters* **201**, 183-186
6. Goldstein, J. L., and Brown, M. S. (1990) *Nature* **343**, 425-430
7. DeBose-Boyd, R. A. (2008) *Cell Res* **18**, 609-621
8. Stone, N. J., Robinson, J. G., Lichtenstein, A. H., Merz, C. N. B., Blum, C. B., Eckel, R. H., Goldberg, A. C., Gordon, D., Levy, D., Lloyd-Jones, D. M., McBride, P., Schwartz, J. S., Shero, S. T., Smith, S. C., Watson, K., and Wilson, P. W. F. (2014) *J Am Coll Cardiol* **63**, 2889-2934
9. Watts, G. F., Gidding, S., Wierzbicki, A. S., Toth, P. P., Alonso, R., Brown, W. V., Bruckert, E., Defesche, J., Lin, K. K., Livingston, M., Mata, P., Parhofer, K. G., Raal, F. J., Santos, R. D., Sijbrands, E. J. G., Simpson, W. G., Sullivan, D. R., Susekov, A. V., Tomlinson, B., Wiegman, A., Yamashita, S., and Kastelein, J. J. P. (2014) *Int J Cardiol* **171**, 309-325
10. Kathiresan, S., Melander, O., Guiducci, C., Surti, A., Burtt, N. P., Rieder, M. J., Cooper, G. M., Roos, C., Voight, B. F., Havulinna, A. S., Wahlstrand, B., Hedner, T., Corella, D., Tai, E. S., Ordovas, J. M., Berglund, G., Vartiainen, E., Jousilahti, P., Hedblad, B., Taskinen, M. R., Newton-Cheh, C., Salomaa, V., Peltonen, L., Groop, L., Altshuler, D. M., and Orho-Melander, M. (2008) *Nat Genet* **40**, 189-197
11. Aulchenko, Y. S., Ripatti, S., Lindqvist, I., Boomsma, D., Heid, I. M., Pramstaller, P. P., Penninx, B. W., Janssens, A. C., Wilson, J. F., Spector, T., Martin, N. G., Pedersen, N. L., Kyvik, K. O., Kaprio, J., Hofman, A., Freimer, N. B., Jarvelin, M. R., Gyllensten, U., Campbell, H., Rudan, I., Johansson, A., Marroni, F., Hayward, C., Vitart, V., Jonasson, I., Pattaro, C., Wright, A., Hastie, N., Pichler, I., Hicks, A. A., Falchi, M., Willemsen, G., Hottenga, J. J., de Geus, E. J., Montgomery, G.

W., Whitfield, J., Magnusson, P., Saharinen, J., Perola, M., Silander, K., Isaacs, A., Sijbrands, E. J., Uitterlinden, A. G., Witteman, J. C., Oostra, B. A., Elliott, P., Ruokonen, A., Sabatti, C., Gieger, C., Meitinger, T., Kronenberg, F., Doring, A., Wichmann, H. E., Smit, J. H., McCarthy, M. I., van Duijn, C. M., and Peltonen, L. (2009) *Nat Genet* **41**, 47-55

12. Burkhardt, R., Kenny, E. E., Lowe, J. K., Birkeland, A., Josowitz, R., Noel, M., Salit, J., Maller, J. B., Pe'er, I., Daly, M. J., Altshuler, D., Stoffel, M., Friedman, J. M., and Breslow, J. L. (2008) *Arterioscler Thromb Vasc Biol* **28**, 2078-2084
13. Hiura, Y., Tabara, Y., Kokubo, Y., Okamura, T., Goto, Y., Nonogi, H., Miki, T., Tomoike, H., and Iwai, N. (2010) *Circ J* **74**, 518-522
14. Freitas, R. N., Khaw, K. T., Wu, K., Bowman, R., Jeffery, H., Luben, R., Wareham, N. J., and Bingham, S. A. (2009) *J Am Soc Hypertens* **3**, 238-244
15. Freitas, R. N., Khaw, K. T., Wu, K., Bowman, R., Jeffery, H., Luben, R., Wareham, N. J., and Rodwell, S. (2010) *Eur J Cardiovasc Prev Rehabil* **17**, 89-93
16. Luo, H., Zhang, X., Shuai, P., Miao, Y., Ye, Z., and Lin, Y. (2017) *J Genet* **96**, 985-992
17. Swerdlow, D. I., Preiss, D., Kuchenbaecker, K. B., Holmes, M. V., Engmann, J. E., Shah, T., Sofat, R., Stender, S., Johnson, P. C., Scott, R. A., Leusink, M., Verweij, N., Sharp, S. J., Guo, Y., Giambartolomei, C., Chung, C., Peasey, A., Amuzu, A., Li, K., Palmen, J., Howard, P., Cooper, J. A., Drenos, F., Li, Y. R., Lowe, G., Gallacher, J., Stewart, M. C., Tzoulaki, I., Buxbaum, S. G., van der, A. D., Forouhi, N. G., Onland-Moret, N. C., van der Schouw, Y. T., Schnabel, R. B., Hubacek, J. A., Kubinova, R., Baceviciene, M., Tamosiunas, A., Pajak, A., Topor-Madry, R., Stepaniak, U., Malyutina, S., Baldassarre, D., Sennblad, B., Tremoli, E., de Faire, U., Veglia, F., Ford, I., Jukema, J. W., Westendorp, R. G., de Borst, G. J., de Jong, P. A., Algra, A., Spiering, W., Maitland-van der Zee, A. H., Klungel, O. H., de Boer, A., Doevendans, P. A., Eaton, C. B., Robinson, J. G., Duggan, D., Consortium, D., Consortium, M., InterAct, C., Kjekshus, J., Downs, J. R., Gotto, A. M., Keech, A. C., Marchioli, R., Tognoni, G., Sever, P. S., Poulter, N. R., Waters, D. D., Pedersen, T. R., Amarenco, P., Nakamura, H., McMurray, J. J., Lewsey, J. D., Chasman, D. I., Ridker, P. M., Maggioni, A. P., Tavazzi, L., Ray, K. K., Seshasai, S. R., Manson, J. E., Price, J. F., Whincup, P. H., Morris, R. W., Lawlor, D. A., Smith, G. D., Ben-Shlomo, Y., Schreiner, P. J., Fornage, M., Siscovick, D. S., Cushman, M., Kumari, M., Wareham, N. J., Verschuren, W. M., Redline, S., Patel, S. R., Whittaker, J. C., Hamsten, A., Delaney, J. A., Dale, C., Gaunt, T. R., Wong, A., Kuh, D., Hardy, R., Kathiresan, S., Castillo, B. A., van der Harst, P., Brunner, E. J., Tybjaerg-Hansen, A., Marmot, M. G., Krauss, R. M., Tsai, M., Coresh, J., Hoogeveen, R. C., Psaty, B. M., Lange, L. A., Hakonarson, H., Dudbridge, F., Humphries, S. E., Talmud, P. J., Kivimaki, M., Timpson, N. J., Langenberg, C., Asselbergs, F. W., Voevoda, M., Bobak, M., Pikhart, H., Wilson, J. G., Reiner, A. P., Keating, B. J., Hingorani, A. D., and Sattar, N. (2015) *Lancet* **385**, 351-361
18. Rosticci, M., Marullo, L., Cicero, A. F., Magi, R., Fischer, K., Pervjakova, N., D'Addato, S., Rizzoli, E., Massimo, G., Giovannini, M., Angelini, S., Scapoli, C., Prokopenko, I., and Borghi, C. (2015) *J Hypertens* **33 Suppl 1**, e3-4

19. Krauss, R. M., Mangravite, L. M., Smith, J. D., Medina, M. W., Wang, D., Guo, X., Rieder, M. J., Simon, J. A., Hulley, S. B., Waters, D., Saad, M., Williams, P. T., Taylor, K. D., Yang, H., Nickerson, D. A., and Rotter, J. I. (2008) *Circulation* **117**, 1537-1544
20. Medina, M. W., Gao, F., Ruan, W., Rotter, J. I., and Krauss, R. M. (2008) *Circulation* **118**, 355-362
21. Thompson, J. F., Hyde, C. L., Wood, L. S., Paciga, S. A., Hinds, D. A., Cox, D. R., Hovingh, G. K., and Kastelein, J. J. (2009) *Circ Cardiovasc Genet* **2**, 173-181
22. Nguyen, A. D., McDonald, J. G., Bruick, R. K., and DeBose-Boyd, R. A. (2007) *J Biol Chem* **282**, 27436-27446
23. Zhang, C. (2008) *Physiol Genomics* **33**, 139-147
24. Krutzfeldt, J., and Stoffel, M. (2006) *Cell Metab* **4**, 9-12
25. Thum, T., Catalucci, D., and Bauersachs, J. (2008) *Cardiovasc Res* **79**, 562-570
26. Najafi-Shoushtari, S. H. (2011) *Curr Atheroscler Rep* **13**, 202-207
27. Chang, T. C., and Mendell, J. T. (2007) *Annu Rev Genomics Hum Genet* **8**, 215-239
28. Nemecz, M., Alexandru, N., Tanko, G., and Georgescu, A. (2016) *Curr Hypertens Rep* **18**, 87
29. Condorelli, G., Latronico, M. V. G., and Cavarretta, E. (2014) *J Am Coll Cardiol* **63**, 2177-2187
30. Gupta, M. P., Gupta, M., Zak, R., and Sukhatme, V. P. (1991) *J Biol Chem.* **266**, 12813-12816
31. Ma, J. J., Ren, Z. J., Ma, Y., Xu, L., Zhao, Y., Zheng, C. G., Fang, Y. H., Xue, T., Sun, B. L., and Xiao, W. H. (2009) *Journal of Biological Chemistry* **284**, 34600-34606
32. Mahapatra, N. R., Mahata, M., Ghosh, S., Gayen, J. R., O'Connor, D. T., and Mahata, S. K. (2006) *J Neurochem* **99**, 119-133
33. Mahapatra, N. R., Mahata, M., O'Connor, D. T., and Mahata, S. K. (2003) *J Biol Chem* **278**, 19986-19994
34. Livak, K. J., and Schmittgen, T. D. (2001) *Methods* **25**, 402-408
35. Dolken, L., Ruzsics, Z., Radle, B., Friedel, C. C., Zimmer, R., Mages, J., Hoffmann, R., Dickinson, P., Forster, T., Ghazal, P., and Koszinowski, U. H. (2008) *Rna* **14**, 1959-1972
36. Tan, L. P., Seinen, E., Duns, G., de Jong, D., Sibon, O. C., Poppema, S., Kroesen, B. J., Kok, K., and van den Berg, A. (2009) *Nucleic Acids Res* **37**, e137
37. Schneider, C. A., Rasband, W. S., and Eliceiri, K. W. (2012) *Nat Methods* **9**, 671-675
38. Peters, L. L., Robledo, R. F., Bult, C. J., Churchill, G. A., Paigen, B. J., and Svenson, K. L. (2007) *Nat Rev Genet* **8**, 58-69
39. Alexiou, P., Maragkakis, M., Papadopoulos, G. L., Reczko, M., and Hatzigeorgiou, A. G. (2009) *Bioinformatics* **25**, 3049-3055
40. Yang, Z., Cappello, T., and Wang, L. (2015) *Acta Pharm Sin B* **5**, 145-150
41. Zidovetzki, R., and Levitan, I. (2007) *Biochim Biophys Acta* **1768**, 1311-1324
42. Gokey, N. G., Lopez-Anido, C., Gillian-Daniel, A. L., and Svaren, J. (2011) *J Biol Chem* **286**, 29501-29510

43. Kucharzewska, P., Christianson, H. C., and Belting, M. (2015) *PLoS One* **10**, e0116740
44. Kulshreshtha, R., Ferracin, M., Wojcik, S. E., Garzon, R., Alder, H., Agosto-Perez, F. J., Davuluri, R., Liu, C. G., Croce, C. M., Negrini, M., Calin, G. A., and Ivan, M. (2007) *Mol Cell Biol* **27**, 1859-1867
45. Xu, Y., Zhou, M., Wang, J., Zhao, Y., Li, S., Zhou, B., Su, Z., Xu, C., Xia, Y., Qian, H., Tu, X., Xiao, W., Chen, X., Chen, Q., and Wang, Q. K. (2014) *Biochim Biophys Acta* **1842**, 712-725
46. Kang, B. Y., Park, K. K., Green, D. E., Bijli, K. M., Searles, C. D., Sutliff, R. L., and Hart, C. M. (2013) *PLoS One* **8**, e79503
47. Lin, Q., Gao, Z., Alarcon, R. M., Ye, J., and Yun, Z. (2009) *Febs j* **276**, 2348-2358
48. Golomb, B. A., and Evans, M. A. (2008) *Am J Cardiovasc Drugs* **8**, 373-418
49. Singh, A. K., Aryal, B., Zhang, X., Fan, Y., Price, N. L., Suarez, Y., and Fernandez-Hernando, C. (2017) *Semin Cell Dev Biol*
50. van Rooij, E., and Kauppinen, S. (2014) *EMBO Mol Med* **6**, 851-864
51. Ference, B. A., Kastelein, J. J. P., Ginsberg, H. N., Chapman, M. J., Nicholls, S. J., Ray, K. K., Packard, C. J., Laufs, U., Brook, R. D., Oliver-Williams, C., Butterworth, A. S., Danesh, J., Smith, G. D., Catapano, A. L., and Sabatine, M. S. (2017) *Jama* **318**, 947-956
52. Selitsky, S. R., Dinh, T. A., Toth, C. L., Kurtz, C. L., Honda, M., Struck, B. R., Kaneko, S., Vickers, K. C., Lemon, S. M., and Sethupathy, P. (2015) *MBio* **6**, e01500-01515
53. Saravanan, N., Patil, M. A., Kumar, P. U., Suryanarayana, P., and Reddy, G. B. (2017) *Indian Journal of Experimental Biology* **55**, 142-150
54. Nishimura, T., and Fabian, M. R. (2016) *Embo Journal* **35**, 1158-1159
55. Bazzini, A. A., Lee, M. T., and Giraldez, A. J. (2012) *Science* **336**, 233-237
56. Ferland-McCollough, D., Fernandez-Twinn, D. S., Cannell, I. G., David, H., Warner, M., Vaag, A. A., Bork-Jensen, J., Brons, C., Gant, T. W., Willis, A. E., Siddle, K., Bushell, M., and Ozanne, S. E. (2012) *Cell Death Differ.* **19**, 1003-1012
57. Daimiel-Ruiz, L., Klett-Mingo, M., Konstantinidou, V., Mico, V., Aranda, J. F., Garcia, B., Martinez-Botas, J., Davalos, A., Fernadez-Hernando, C., and Ordovas, J. M. (2015) *Mol Nutr Food Res.* **59**, 1865-1878
58. Christy, B., and Nathans, D. (1989) *Proc Natl Acad Sci U S A* **86**, 8737-8741
59. Fu, M., Zhu, X., Zhang, J., Liang, J., Lin, Y., Zhao, L., Ehrengruber, M. U., and Chen, Y. E. (2003) *Gene* **315**, 33-41
60. Khachigian, L. M. (2006) *Circ Res* **98**, 186-191
61. Mohn, K. L., Laz, T. M., Melby, A. E., and Taub, R. (1990) *J Biol Chem.* **265**, 21914-21921
62. Devaux, Y., Vausort, M., McCann, G. P., Kelly, D., Collignon, O., Ng, L. L., Wagner, D. R., and Squire, I. B. (2013) *PLoS One* **8**, e70644
63. Chen, W. J., Yin, K., Zhao, G. J., Fu, Y. C., and Tang, C. K. (2012) *Atherosclerosis* **222**, 314-323
64. Brown, M. S., and Goldstein, J. L. (2009) *J Lipid Res* **50**, 1255-1255

65. Sharpe, L. J., Cook, E. C., Zelcer, N., and Brown, A. J. (2014) *Trends Biochem Sci* **39**, 527-535
66. Horton, J. D., Goldstein, J. L., and Brown, M. S. (2002) *J Clin Invest* **109**, 1125-1131
67. Brown, A. J., Sun, L., Feramisco, J. D., Brown, M. S., and Goldstein, J. L. (2002) *Mol Cell* **10**, 237-245
68. Song, B. L., and DeBose-Boyd, R. A. (2004) *J Biol Chem* **279**, 28798-28806
69. Vickers, K. C., Shoucri, B. M., Levin, M. G., Wu, H., Pearson, D. S., Osei-Hwedieh, D., Collins, F. S., Remaley, A. T., and Sethupathy, P. (2013) *Hepatology* **57**, 533-542
70. Alisi, A., Da Sacco, L., Bruscalupi, G., Piemonte, F., Panera, N., De Vito, R., Leoni, S., Bottazzo, G. F., Masotti, A., and Nobili, V. (2011) *Lab Invest.* **91**, 283-293
71. Karolina, D. S., Tavintharan, S., Armugam, A., Sepramaniam, S., Pek, S. L. T., Wong, M. T. K., Lim, S. C., Sum, C. F., and Jeyaseelan, K. (2012) *J Clin Endocrinol Metab.* **97**, E2271-E2276
72. Burgueno, A. L., Gianotti, T. F., Mansilla, N. G., Pirola, C. J., and Sookoian, S. (2013) *Clin Sci (Lond)* **124**, 53-63
73. Cao, R., Zhao, X., Li, S., Zhou, H., Chen, W., Ren, L., Zhou, X., Zhang, H., and Shi, R. (2014) *Cell Physiol Biochem* **34**, 1427-1441
74. Li, J., Thorne, L. N., Punjabi, N. M., Sun, C. K., Schwartz, A. R., Smith, P. L., Marino, R. L., Rodriguez, A., Hubbard, W. C., O'Donnell, C. P., and Polotsky, V. Y. (2005) *Circ Res* **97**, 698-706
75. Zhang, P., Tchou-Wong, K. M., and Costa, M. (2007) *Cancer Research* **67**, 9125-9133
76. Sperandio, S., Fortin, J., Sasik, R., Robitaille, L., Corbeil, J., and de Belle, I. (2009) *Mol Carcinog* **48**, 38-44
77. Xie, W., Li, L., Zhang, M., Cheng, H. P., Gong, D., Lv, Y. C., Yao, F., He, P. P., Ouyang, X. P., Lan, G., Liu, D., Zhao, Z. W., Tan, Y. L., Zheng, X. L., Yin, W. D., and Tang, C. K. (2016) *PLoS One* **11**, e0157085

Fig.1

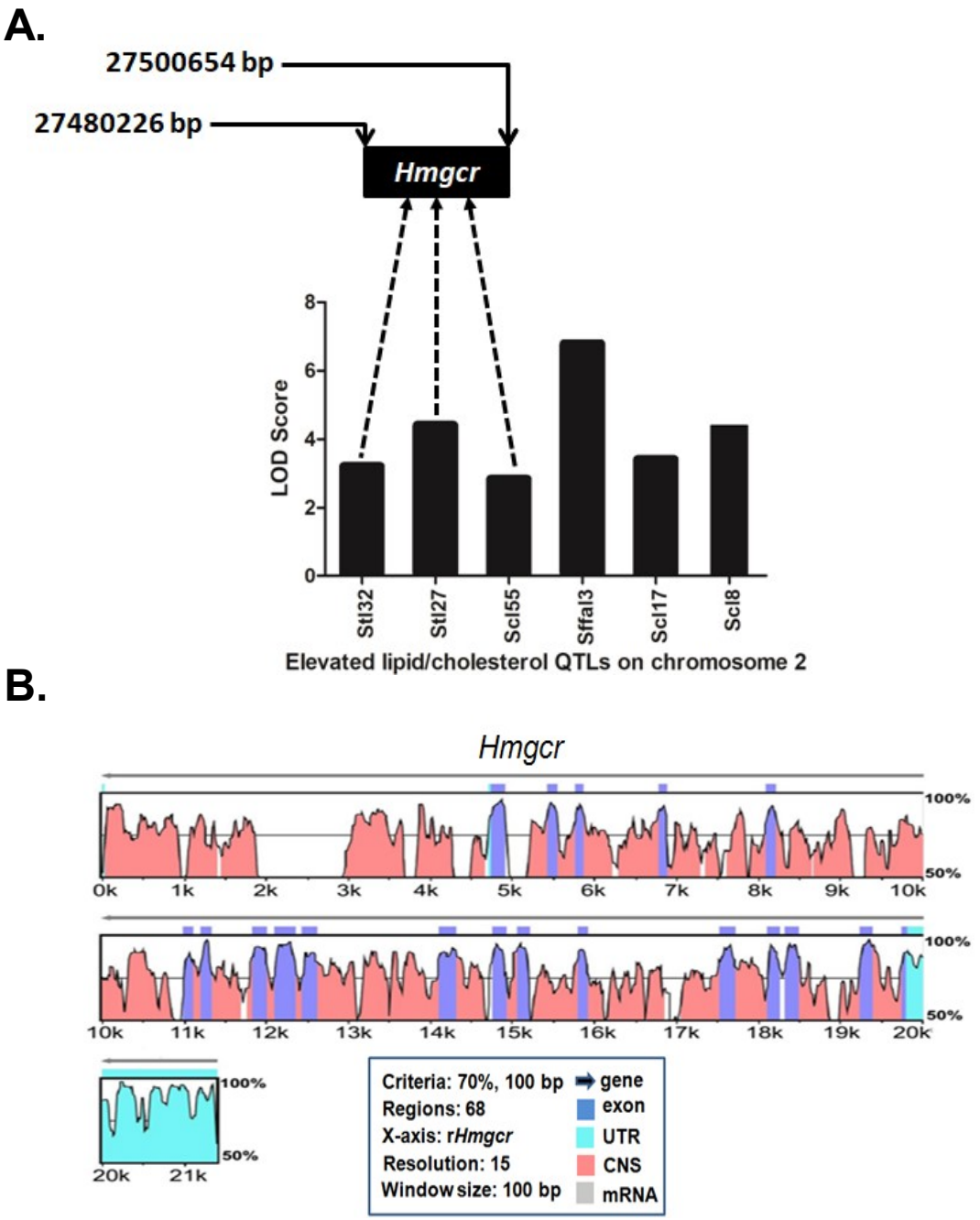
A.
27500654 bp
27480226 bp
Hmgcr
LOD Score
8
6
4
2
0
Stl32
Stl27
Scl55
Sffal3
Scl17
Scl8
Elevated lipid/cholesterol QTLs on chromosome 2
B.
Hmgcr
100%
50%
0k
1k
2k
3k
4k
5k
6k
7k
8k
9k
10k
10k
11k
12k
13k
14k
15k
16k
17k
18k
19k
20k
20k
21k
Criteria: 70%, 100 bp
Regions: 68
X-axis: rHmgcr
Resolution: 15
Window size: 100 bp
gene
exon
UTR
CNS
mRNA

Fig.2

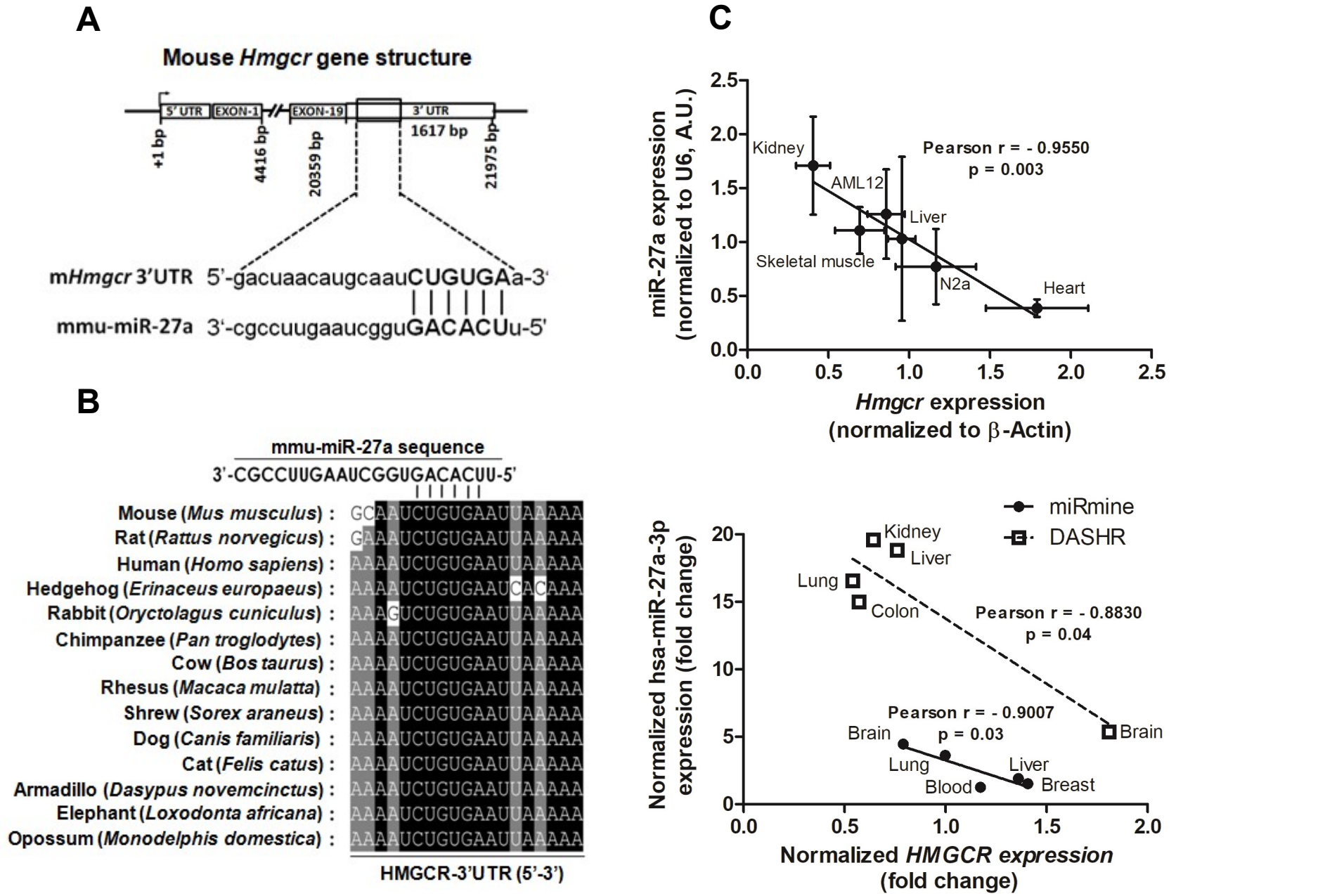
A
Mouse Hmgcr gene structure
5' UTR
EXON-1
EXON-19
3' UTR
+1 bp
4416 bp
20359 bp
1617 bp
21975 bp
mHmgcr 3'UTR 5'-gacuaacaugcaauCUGUGAa-3'
mmu-miR-27a 3'-cgccuugaaucgguGACACUu-5'
B
mmu-miR-27a sequence
3'-CGCCUUGAAUCGGUGACACUU-5'
Mouse (Mus musculus) :
Rat (Rattus norvegicus) :
Human (Homo sapiens) :
Hedgehog (Erinaceus europaeus) :
Rabbit (Oryctolagus cuniculus) :
Chimpanzee (Pan troglodytes) :
Cow (Bos taurus) :
Rhesus (Macaca mulatta) :
Shrew (Sorex araneus) :
Dog (Canis familiaris) :
Cat (Felis catus) :
Armadillo (Dasypus novemcinctus) :
Elephant (Loxodonta africana) :
Opossum (Monodelphis domestica) :
HMGCR-3'UTR (5'-3')
C
miR-27a expression (normalized to U6, A.U.)
Hmgcr expression (normalized to β-Actin)
Kidney
AML12
Liver
Skeletal muscle
N2a
Heart
Pearson r = - 0.9550
p = 0.003
Normalized hsa-miR-27a-3p expression (fold change)
Normalized HMGCR expression (fold change)
miRmine
DASHR
Kidney
Liver
Lung
Colon
Brain
Pearson r = - 0.8830
p = 0.04
Pearson r = - 0.9007
p = 0.03
Brain
Lung
Liver
Blood
Breast

Fig.3

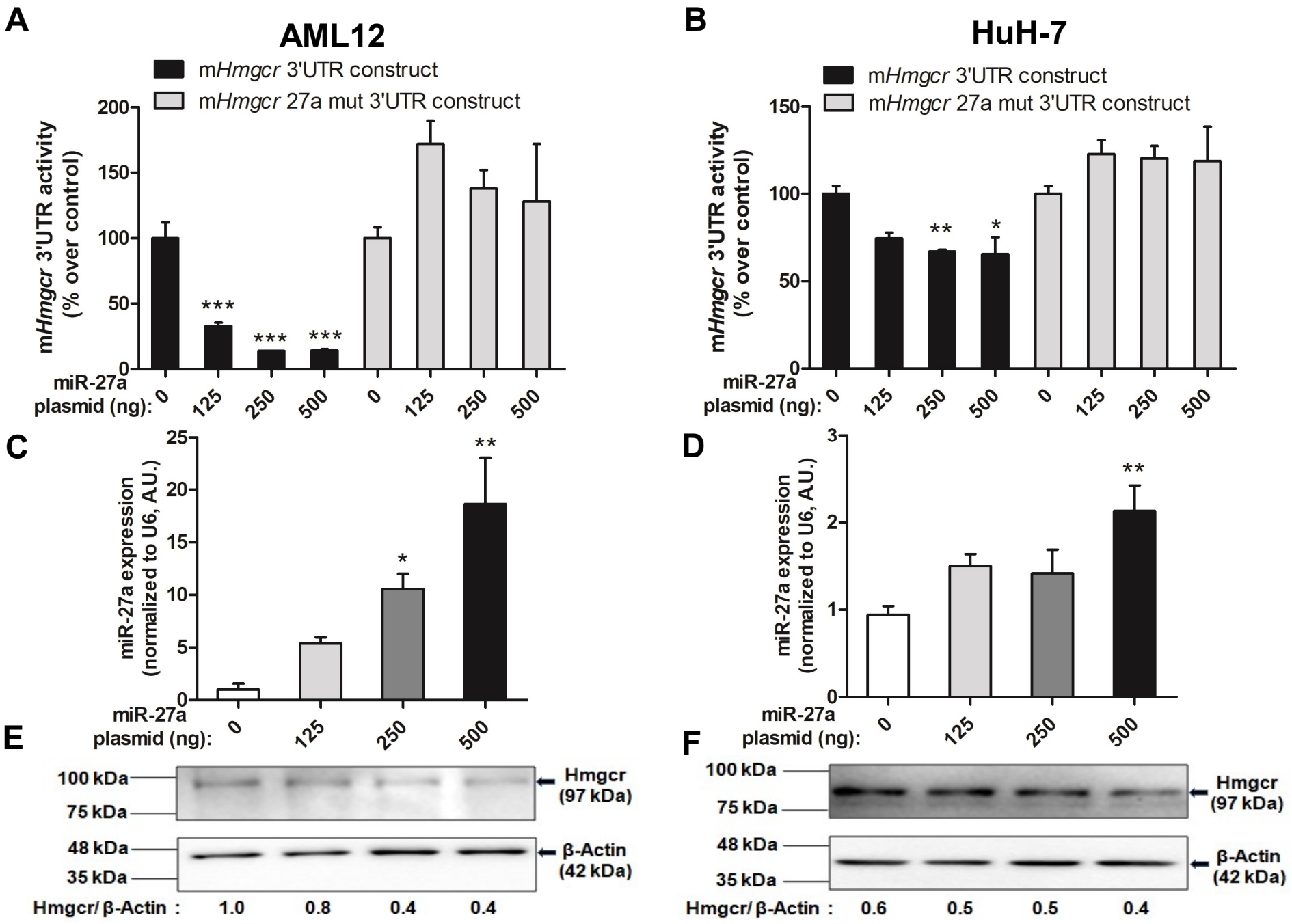
A
AML12
mHmgcr 3'UTR construct
mHmgcr 27a mut 3'UTR construct
mHmgcr 3'UTR activity (% over control)
200
150
100
50
0
***
***
***
miR-27a plasmid (ng):
0
125
250
500
0
125
250
500
B
HuH-7
mHmgcr 3'UTR construct
mHmgcr 27a mut 3'UTR construct
mHmgcr 3'UTR activity (% over control)
150
100
50
0
**
*
miR-27a plasmid (ng):
0
125
250
500
0
125
250
500
C
miR-27a expression (normalized to U6, A.U.)
25
20
15
10
5
0
*
**
miR-27a plasmid (ng):
0
125
250
500
D
miR-27a expression (normalized to U6, A.U.)
3
2
1
0
**
miR-27a plasmid (ng):
0
125
250
500
E
100 kDa
75 kDa
Hmgcr (97 kDa)
48 kDa
35 kDa
β-Actin (42 kDa)
Hmgcr/ β-Actin :
1.0
0.8
0.4
0.4
F
100 kDa
75 kDa
Hmgcr (97 kDa)
48 kDa
35 kDa
β-Actin (42 kDa)
Hmgcr/ β-Actin :
0.6
0.5
0.5
0.4

Fig.4

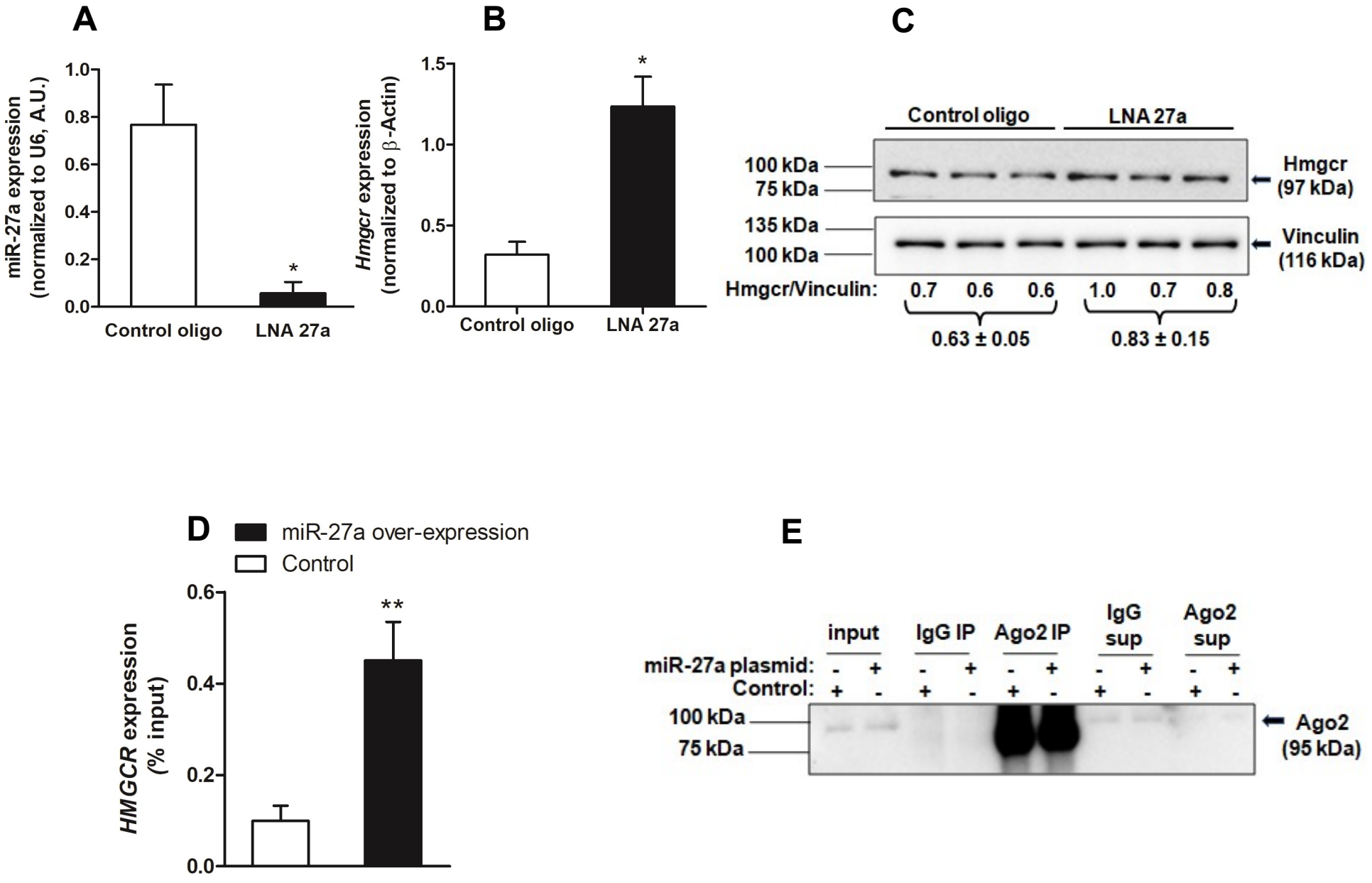
A
miR-27a expression (normalized to U6, A.U.)
1.0
0.8
0.6
0.4
0.2
0.0
*
Control oligo
LNA 27a
B
Hmgcr expression (normalized to β-Actin)
1.5
1.0
0.5
0.0
*
Control oligo
LNA 27a
C
Control oligo
LNA 27a
100 kDa
75 kDa
Hmgcr (97 kDa)
135 kDa
100 kDa
Vinculin (116 kDa)
Hmgcr/Vinculin:
0.7 0.6 0.6
1.0 0.7 0.8
0.63 ± 0.05
0.83 ± 0.15
D
miR-27a over-expression
Control
HMGCR expression (% input)
0.6
0.4
0.2
0.0
**
E
input
IgG IP
Ago2 IP
IgG sup
Ago2 sup
miR-27a plasmid: - + - + - + - + - +
Control: + - + - + - + - + -
100 kDa
75 kDa
Ago2 (95 kDa)

Fig.5

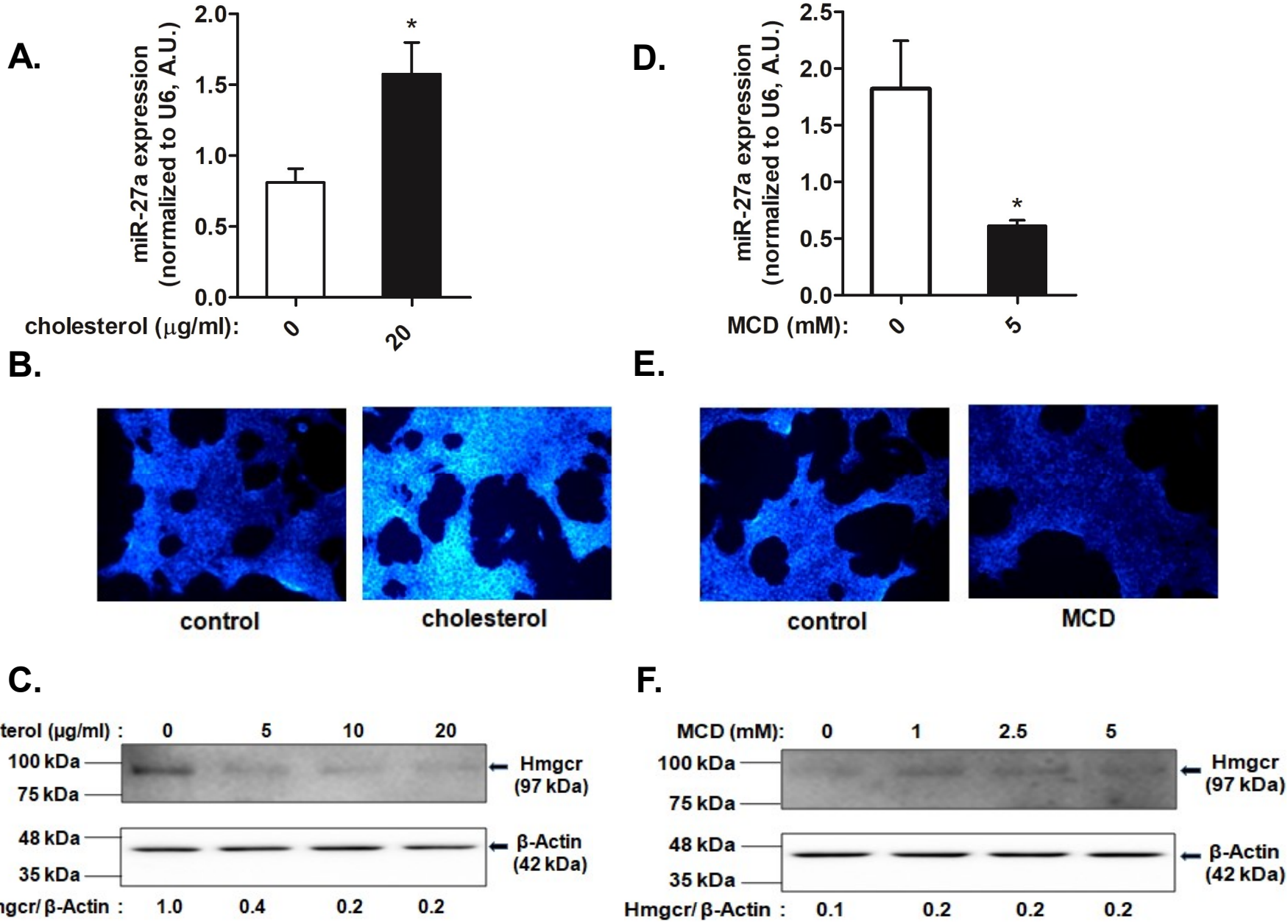
A.
miR-27a expression (normalized to U6, A.U.)
2.0
1.5
1.0
0.5
0.0
*
cholesterol (μg/ml):
0
20
D.
miR-27a expression (normalized to U6, A.U.)
2.5
2.0
1.5
1.0
0.5
0.0
*
MCD (mM):
0
5
B.
control
cholesterol
E.
control
MCD
C.
cholesterol (μg/ml) :
0
5
10
20
100 kDa
75 kDa
Hmgcr (97 kDa)
48 kDa
35 kDa
β-Actin (42 kDa)
Hmgcr/ β-Actin :
1.0
0.4
0.2
0.2
F.
MCD (mM):
0
1
2.5
5
100 kDa
75 kDa
Hmgcr (97 kDa)
48 kDa
35 kDa
β-Actin (42 kDa)
Hmgcr/ β-Actin :
0.1
0.2
0.2
0.2

Fig.6

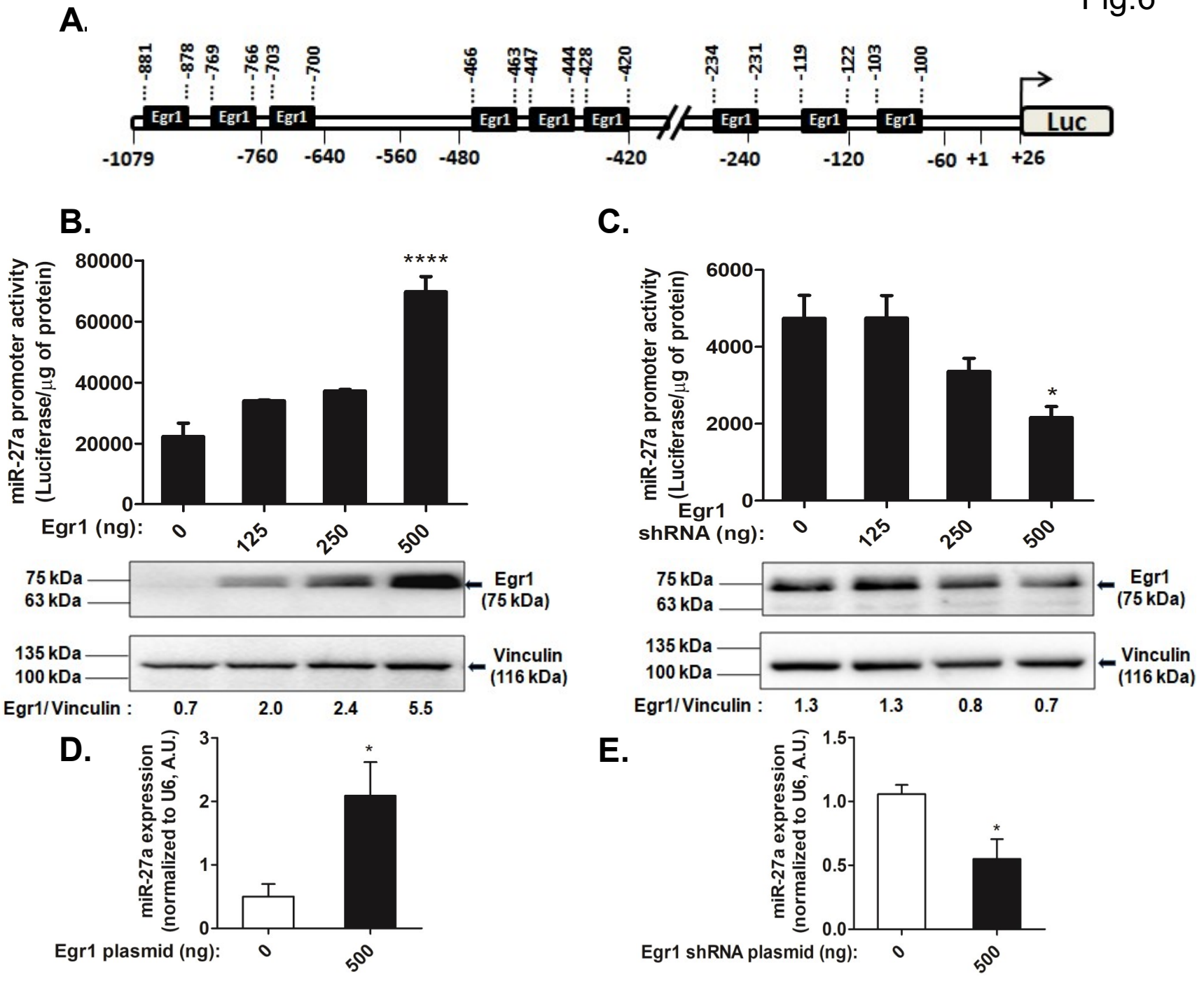
A.
-881
-878
-769
-766
-703
-700
-466
-463
-447
-444
-428
-420
-234
-231
-119
-122
-103
-100
Egr1
Luc
-1079
-760
-640
-560
-480
-420
-240
-120
-60
+1
+26
B.
miR-27a promoter activity (Luciferase/μg of protein)
80000
60000
40000
20000
0
****
Egr1 (ng):
0
125
250
500
75 kDa
63 kDa
Egr1 (75 kDa)
135 kDa
100 kDa
Vinculin (116 kDa)
Egr1/ Vinculin :
0.7
2.0
2.4
5.5
C.
miR-27a promoter activity (Luciferase/μg of protein)
6000
4000
2000
0
*
Egr1 shRNA (ng):
0
125
250
500
75 kDa
63 kDa
Egr1 (75 kDa)
135 kDa
100 kDa
Vinculin (116 kDa)
Egr1/ Vinculin :
1.3
1.3
0.8
0.7
D.
miR-27a expression (normalized to U6, A.U.)
3
2
1
0
*
Egr1 plasmid (ng):
0
500
E.
miR-27a expression (normalized to U6, A.U.)
1.5
1.0
0.5
0.0
*
Egr1 shRNA plasmid (ng):
0
500

Fig.7

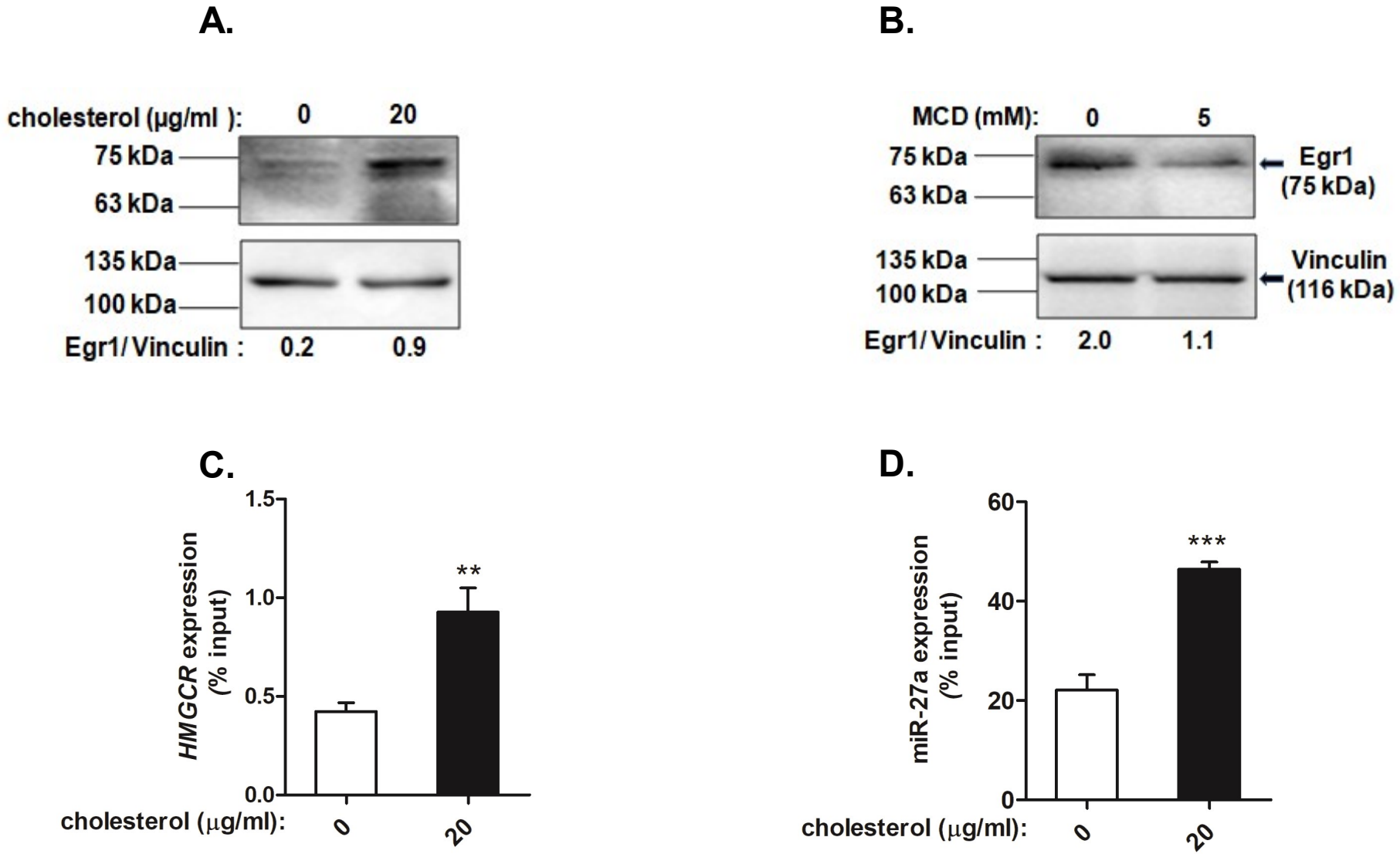
A.
cholesterol (μg/ml): 0 20
75 kDa
63 kDa
135 kDa
100 kDa
Egr1/ Vinculin : 0.2 0.9
B.
MCD (mM): 0 5
75 kDa
63 kDa
Egr1 (75 kDa)
135 kDa
100 kDa
Vinculin (116 kDa)
Egr1/ Vinculin : 2.0 1.1
C.
HMGCR expression (% input)
1.5
1.0
0.5
0.0
**
cholesterol (μg/ml): 0 20
D.
miR-27a expression (% input)
60
40
20
0
***
cholesterol (μg/ml): 0 20

Fig.8

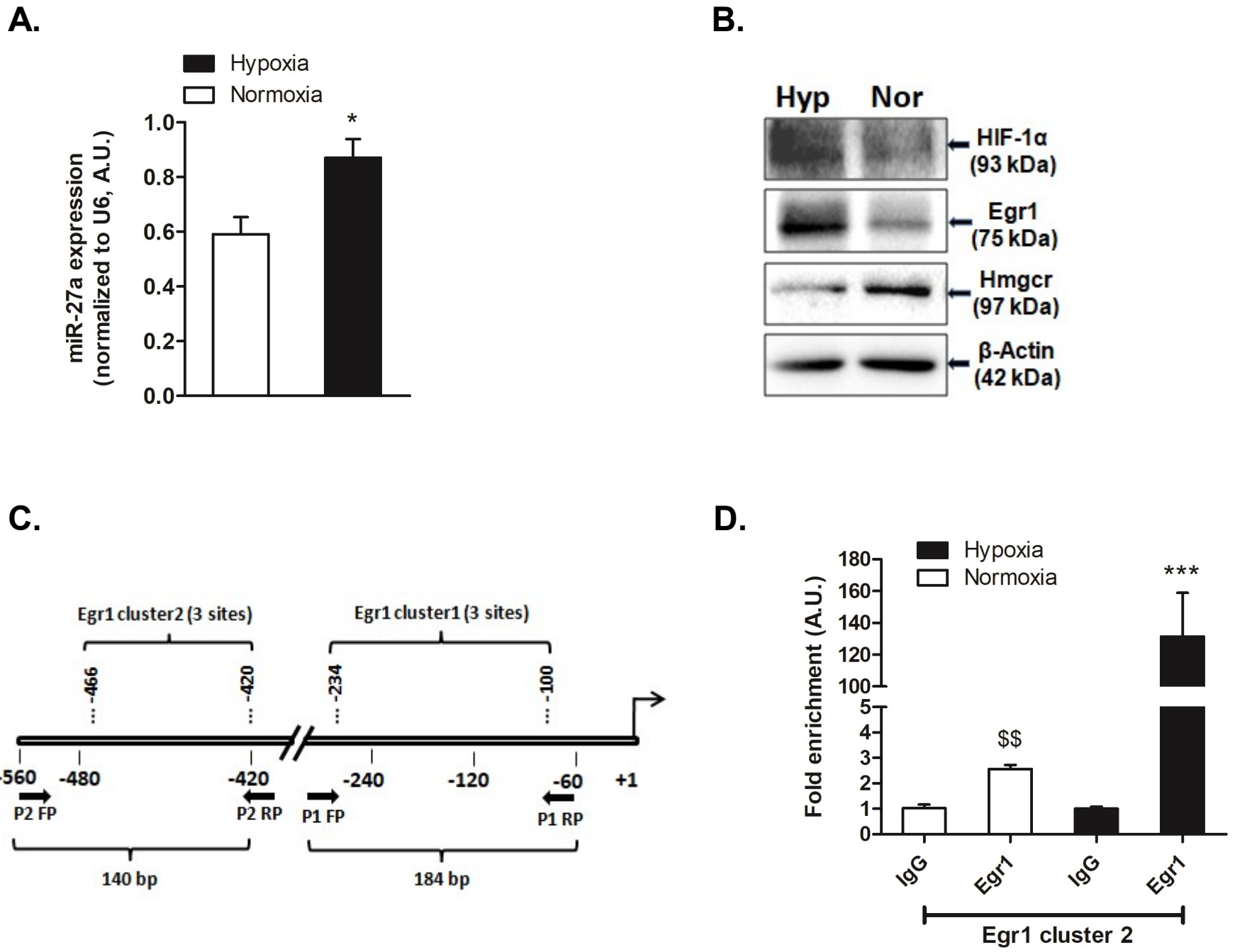
A.
Hypoxia
Normoxia
miR-27a expression (normalized to U6, A.U.)
1.0
0.8
0.6
0.4
0.2
0.0
*
B.
Hyp
Nor
HIF-1α (93 kDa)
Egr1 (75 kDa)
Hmgcr (97 kDa)
β-Actin (42 kDa)
C.
Egr1 cluster2 (3 sites)
Egr1 cluster1 (3 sites)
-466
-420
-234
-100
-560
-480
-420
-240
-120
-60
+1
P2 FP
P2 RP
P1 FP
P1 RP
140 bp
184 bp
D.
Hypoxia
Normoxia
Fold enrichment (A.U.)
180
160
140
120
100
5
4
3
2
1
0
***
$$
IgG
Egr1
IgG
Egr1
Egr1 cluster 2

Fig.9

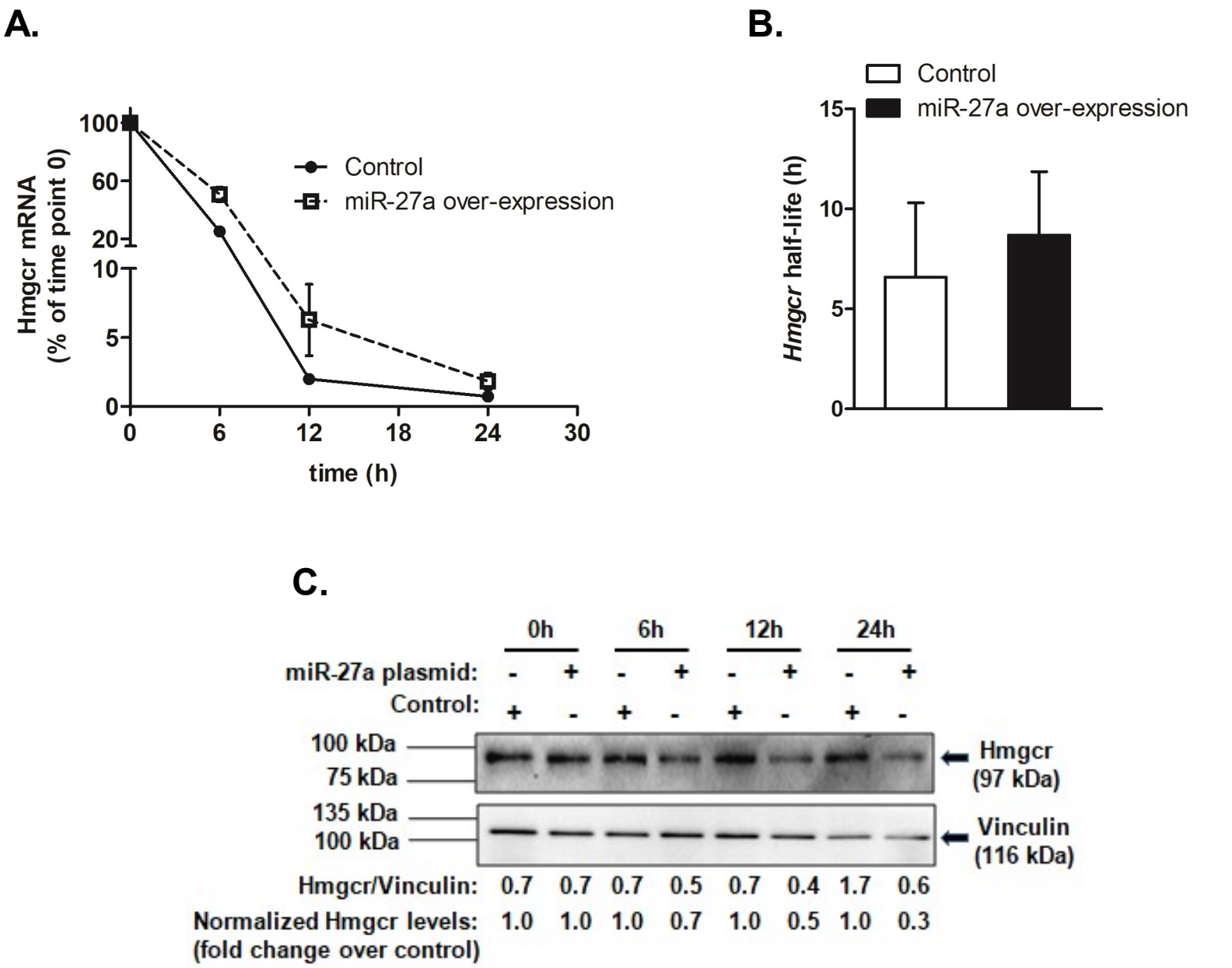
A.
Hmgcr mRNA (% of time point 0)
100
60
20
10
5
0
0
6
12
18
24
30
time (h)
Control
miR-27a over-expression
B.
Hmgcr half-life (h)
15
10
5
0
Control
miR-27a over-expression
C.
0h
6h
12h
24h
miR-27a plasmid: - + - + - + - +
Control: + - + - + - + -
100 kDa
75 kDa
135 kDa
100 kDa
Hmgcr (97 kDa)
Vinculin (116 kDa)
Hmgcr/Vinculin: 0.7 0.7 0.7 0.5 0.7 0.4 1.7 0.6
Normalized Hmgcr levels: 1.0 1.0 1.0 0.7 1.0 0.5 1.0 0.3
(fold change over control)

Fig.10

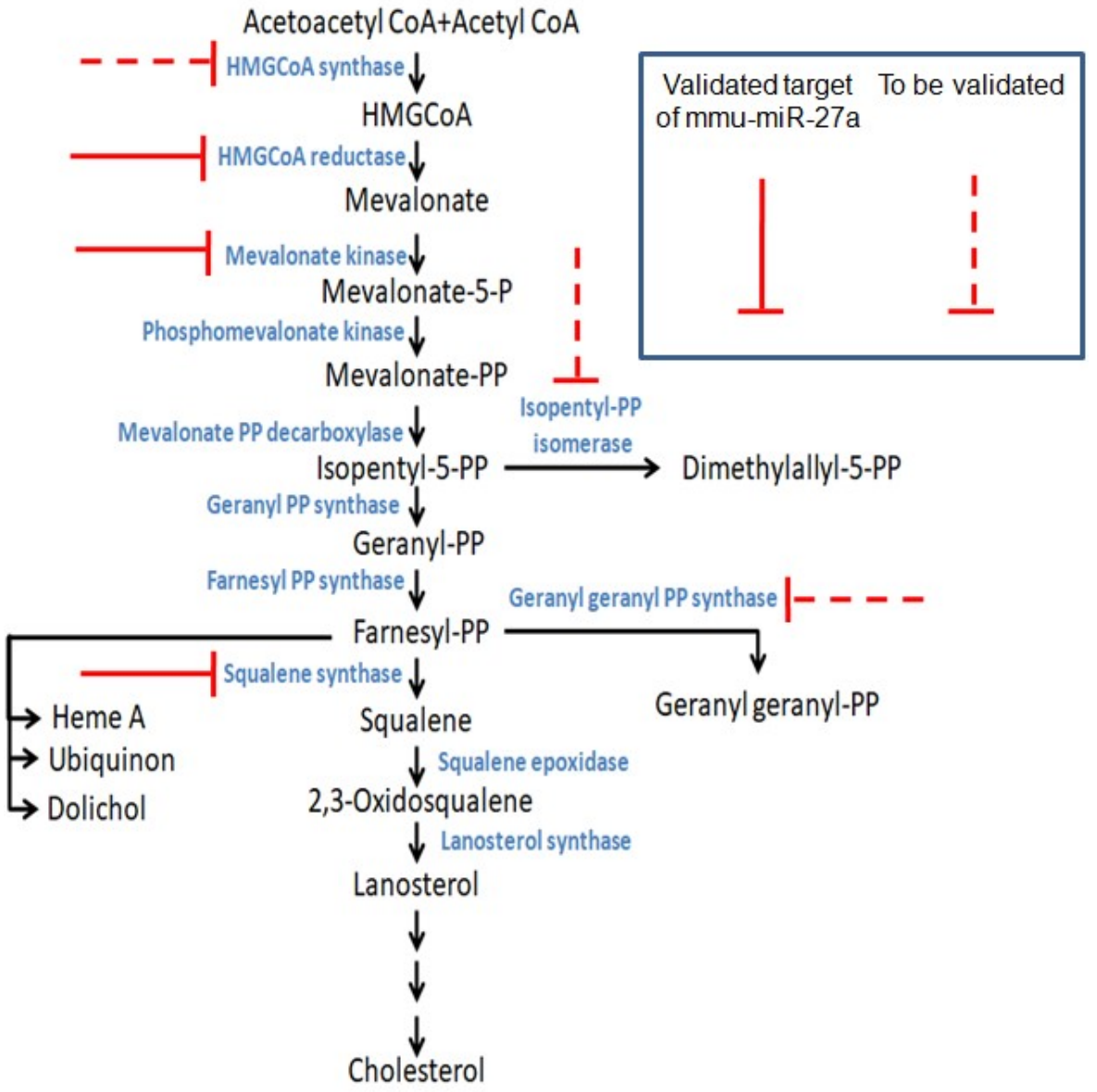
Acetoacetyl CoA+Acetyl CoA
HMGCoA synthase
HMGCoA
HMGCoA reductase
Mevalonate
Mevalonate kinase
Mevalonate-5-P
Phosphomevalonate kinase
Mevalonate-PP
Mevalonate PP decarboxylase
Isopentyl-PP isomerase
Isopentyl-5-PP
Dimethylallyl-5-PP
Geranyl PP synthase
Geranyl-PP
Farnesyl PP synthase
Geranyl geranyl PP synthase
Farnesyl-PP
Squalene synthase
Geranyl geranyl-PP
Heme A
Ubiquinon
Dolichol
Squalene
Squalene epoxidase
2,3-Oxidosqualene
Lanosterol synthase
Lanosterol
Cholesterol
Validated target of mmu-miR-27a
To be validated